NASA CONTRACTOR REPORT

UACRL D-920243-18
NASA CR-54790

INVESTIGATION OF COLLISION PROBABILITY OF ELECTRONS AND IONS WITH ALKALI METAL ATOMS

PREPARED BY R. H. BULLIS AND W. L. NIGHAN

GPO PRICE $ _____

CFSTI PRICE(S) $ _____

Hard copy (HC) 3.00

Microfiche (MF) .50

ff 653 July 65

FACILITY FORM 602

N66-11237 (ACCESSION NUMBER)

(THRU)

51 (PAGES)

1 (CODE)

CR-54790 (NASA CR OR TMX OR AD NUMBER)

25 (CATEGORY)

SEMIANNUAL REPORT
NOVEMBER 1965

PREPARED UNDER CONTRACT NO. NAS 3-4171

BY

United Aircraft Research Laboratories

UNITED AIRCRAFT CORPORATION

EAST HARTFORD, CONNECTICUT

FOR

NATIONAL AERONAUTICS & SPACE ADMINISTRATION
LEWIS RESEARCH CENTER
CLEVELAND, OHIO

NOTICE

This report was prepared as an account of Government-sponsored work. Neither the United States nor the National Aeronautics and Space Administration (NASA), nor any person acting on behalf of NASA:

A) Makes any warranty or representation, expressed or implied, with respect to the accuracy, completeness, or usefulness of the information contained in this report, or that the use of any information, apparatus, method, or process disclosed in this report may not infringe privately-owned rights; or

B) Assumes any liabilities with respect to the use of, or for damages resulting from the use of any information, apparatus, method or process disclosed in this report.

As used above, "person acting on behalf of NASA" includes any employee or contractor of NASA, or employee of such contractor, to the extent that such employee or contractor of NASA or employee of such contractor prepares, disseminates, or provides access to, any information pursuant to his employment or contract with NASA, or his employment with such contractors.

Requests for copies of this report should be referred to

National Aeronautics and Space Administration
Office of Scientific and Technical Information
Washington 25, D. C.
Attention: AFSS-A

UNITED AIRCRAFT CORPORATION
RESEARCH LABORATORIES
East Hartford, Connecticut

NASA Report No.: CR-54790
United Aircraft Corporation Research Laboratories Report No.: D-920243-18
Semiannual Report
Date of Reporting Period: April 22, 1965, to October 21, 1965

Title of Contract: Investigation of Collision Probability of Electrons and Ions with Alkali Metal Atoms

Contract Number: NAS3-4171

Contractor: United Aircraft Corporation Research Laboratories
East Hartford, Connecticut
203-565-4321
Principal Investigator: R. H. Bullis

National Aeronautics and Space Administration
Lewis Research Center
Space Power Systems Division
Project Manager: Mr. H. E. Nastelin, MS 500-309

Reported By: R. H. Bullis
R. H. Bullis

W. L. Nighan
W. L. Nighan

Approved By: Harlan D. Taylor
Harlan D. Taylor
Manager, Physics Department

Date: November 26, 1965

Report D-920243-18

Semiannual Report under Contract NAS3-4171
for the Period April 22, 1965, through October 21, 1965

Investigation of Collision Probability of Electrons and Ions with Alkali Metal Atoms

TABLE OF CONTENTS

	Page
SUMMARY	1
ELECTRON-CESIUM ATOM COLLISION PROBABILITY MEASUREMENTS	3
Introduction	3
Description of the Experiment	3
Method of Determining Electron Beam Energy	4
Analysis of Electron-Atom Total Collision Cross Sections	6
Outline of Research for the Next Six-Month Period	9
CESIUM ION-CESIUM ATOM COLLISION PROBABILITY MEASUREMENTS	10
Introduction	10
Cesium Pressure Determinations	11
Analysis of Elastic Scattering Cross Sections	13
Outline of Research for the Next Six-Month Period	15
REFERENCES	16
LIST OF FIGURES	17
FIGURES	18
APPENDIX I	I-1 - 17

Report D-920243-18

Investigation of Collision Probability of Electrons and Ions with Alkali Metal Atoms

Semiannual Progress Report - April 22, 1965, to October 21, 1965

Contract NAS3-4171

Summary

This report contains a summary of the experimental research investigations conducted at the United Aircraft Research Laboratories to determine the collision probabilities of electrons and cesium ions with cesium atoms during the third six-month period from April 22, 1965, through October 21, 1965, under Contract NAS3-4171.

In the first year of the contract, the collision probability of electrons with cesium atoms was determined over an energy range from 0.2 to 0.6 eV by measuring the transport properties of the cesium plasma existing in the positive column of a cesium arc discharge with electrostatic probe and rf conductivity coil diagnostic techniques. The total cesium ion-cesium atom collision probability data previously obtained by beam techniques in a modified Ramsauer cross-section experiment under Contract NASr-112 were analyzed to determine low energy cesium ion mobilities, and further investigations of the low energy cesium ion-cesium atom collision cross sections were made in an effort to extend the energy range of these measurements. In the course of these investigations, ion beams with energies as low as 0.058 eV were detected successfully. The results of the ion mobility analysis were reported at the IEEE Thermionic Conversion Specialist Conference held in Cleveland, Ohio, on October 26 through 28, 1964, and the over-all results of both the electron-cesium atom and the cesium ion-cesium atom collision probability measurements were reported in two papers presented at the Fourth International Conference on the Physics of Electronic and Atomic Collisions held in Quebec, Canada, on August 2 through 6, 1965.

In this current report period design and construction has been initiated on a low energy electron beam experimental apparatus similar in concept to the modified Ramsauer system employed in the cesium ion-cesium atom cross-section measurements. This system will be used to measure the total collision cross section of electrons interacting with cesium atoms over an energy range from 0.5 to 2.5 eV. The most critical portion of this experiment, the design of which has been completed, is the development of a region free of stray magnetic fields and the generation of uniform magnetic fields with intensities of 0.1 gauss for energy analysis of the electron beam. Measurements of the time required for the neutral cesium density in a scattering chamber to reach equilibrium after a temperature change occurs in the cesium reservoir have been made with a surface ionization gauge detector. An analysis has been conducted to determine the effect of using a 4-6-12 type interaction

potential rather than only an inverse fourth power potential to determine the magnitude of the contribution of elastic scattering events to the measured total cesium ion-cesium atom collision cross section. The available experimental electron-atom and electron-molecule differential scattering cross sections reported in the literature have been analyzed in an effort to determine the magnitude of the difference that can exist between the total and momentum transfer cross sections due to anisotropic scattering effects.

A knowledge of both the collision probability of electrons and cesium ions with cesium atoms is of extreme importance in the analysis of the neutralization plasma existing in the ignited-mode thermionic converter. This is illustrated by the many theoretical analyses that are presently being reported in the literature which use this information. A knowledge of these cross sections is also applicable in the analyses of devices other than the converter which employ cesium vapor in an ionized state.

ELECTRON-CESIUM ATOM COLLISION PROBABILITY MEASUREMENTS

Introduction

The cross section for electron-cesium atom momentum transfer collisions, which plays a dominant role in the determination of the transport properties of slightly and partially ionized cesium plasmas, has been determined in the first year of this contract by measuring the transport properties of the cesium plasma that exist in the positive column of a cesium arc discharge. In this measurement, which is essentially a swarm-type experiment, the velocity dependence of the electron-cesium atom momentum transfer collision cross section was determined from the measured averaged effective collision frequency by numerically integrating the electron velocity distribution over the velocity dependence of the cross section. As outlined in detail in Appendix I, which is a preprint of the electron-cesium atom collision probability paper presented at the Fourth International Conference on the Physics of Electronic and Atomic Collisions held in Quebec, Canada, on August 2 through 6, 1965, it is possible by numerical techniques to determine the general behavior of the velocity dependence of the cross section but not the fine structure associated with this velocity dependence. Since these measurements were made over the energy range from 0.2 to 0.6 eV, further cross-section information obtained by beam techniques in the region above 0.5 eV would serve as a natural complement to these earlier measurements and would also increase the range over which the velocity dependence of the cross section is known. Brode,[1] over thirty years ago using beam techniques, measured the total electron-cesium atom collision cross section down to energies of 0.6 eV. However, it is not entirely clear that contact potential effects which can produce large uncertainties in the determination of the energy of the electron beam were eliminated in these measurements. It has been conclusively shown in low energy cesium ion-cesium atom measurements that as much as 2.5 eV uncertainty can exist in the determination of ion beam energies if contact potential effects are not taken into account.[2]

Therefore, the object of this experiment is to measure the total electron-cesium atom cross section over an energy range from 0.5 to 2.5 eV in a system which employs an electroformed collision chamber similar in design to those used in the low energy cesium ion-cesium atom measurements to eliminate uncertainties in the determination of the electron beam energy.

Description of Experiment

In this experiment which is similar in nature to the earlier measurements of Brode,[1] the energy of the electron beam is determined by measuring the radius of curvature of the electron beam in a magnetic field of known intensity. This technique is similar to the technique used in the measurements of low energy cesium ion-cesium atom interactions. In contrast to the earlier measurements of Brode, the uncertainty in the energy determination of the electron beam produced by

contact potential effects is eliminated in these measurements by employing an electroformed collision chamber. As in the ion measurements a scattering event which produces a deflection of the electron beam which is greater than the minimum resolution of the scattering chamber will be counted as a collisional event. The cross section is determined by measuring the attenuation of the electron beam produced by increases in neutral cesium pressure in the collision chamber. This attenuation can be given by

$$I = I_o e^{-p_o P_t x} \tag{1}$$

where

I is the electron beam current exiting the collision chamber for a finite pressure in the chamber.

I_o is the electron beam current exiting the collision chamber for zero pressure in the chamber.

p_o is the pressure in the collision chamber reduced to 273°K.

P_t is the number of collisions per cm of path per mm of pressure.

x is the path length of the electron beam through the chamber.

The total collision cross section is determined by gradually increasing the cesium pressure in the collision chamber and measuring the attenuation of the electron beam intensity produced by the increase in chamber pressure. As Eq. 1 indicates, only a relative measurement of the intensity of the electron beam is required to determine the magnitude of the cross section. At energies above 1.4 eV the electrons in the beam have sufficient energy to be lost from the beam by inelastic, excitation-type collisions. Lastly, it should be noted that in this measurement there is no way to determine whether or not the electron scattering is truly isotropic.

Method of Determining Electron Beam Energy

The electron beam energy is determined uniquely in these measurements from the radius of curvature determined by the geometry of the electroformed collision chamber and the magnitude of the applied magnetic field. Since the collision chamber slits have a finite width, the electron beam focused through the collision chamber has a finite energy width which is determined purely by the geometry of the collision chamber. Since it has been shown in the cesium ion-cesium atom cross-section measurements that the ion beam intensity focused through the chamber is essentially space-charge limited, it would be expected that an increase proportional to the square root of the electron-to-ion mass ratio, which is 500 for the

case of cesium, could be focused through the collision chamber. With higher current levels available the width of the collision chamber slits can be reduced, thereby affecting an improvement in the energy resolution of the system.

In a Ramsauer-type experiment the length of the path of the charged particle beam in the collision chamber required to detect a scattering event is determined by the magnitude of the cross section and the pressure of the scattering gas in the collision chamber. In this type of experiment the neutral pressure in the collision chamber is maintained below the transition regime between free molecular and viscous flow, so that the loss rate of neutral atoms from the entrance and exit slits of the chamber is minimized. On the basis of the pressure limitations and the estimated magnitude of the electron-cesium atom total collision cross section, it was found that the collision chamber for the electron-cesium atom measurements could not be reduced in size from the one used in the cesium ion-cesium atom measurements, even though a reduction in the radius of the electron beam trajectory would be advantageous from the standpoint of the requirements of the magnetic intensity employed for energy selection. Therefore, due to the long beam path length restriction, the required energy selection magnetic fields used in these measurements must be significantly lower in intensity than those used in the ion cross-section measurements.

Generation of Low-Intensity Magnetic Fields

At electron beam energies of 0.5 eV, magnetic field intensities required for energy selection are 0.1 gauss. Since the earth's magnetic field intensity is 0.6 gauss, the generation and detection of fields of this intensity presents a considerable problem, especially in an environment in which the earth's field is perturbed significantly by the presence of structural steel and by heavy laboratory equipment. In the type of energy-selection system employed in this experiment, the uncertainty in the determination of electron beam energy is directly proportional to the square of the uncertainty in the determination of the magnetic field intensity. On this basis the accuracy to which the magnetic field must be generated and measured is 10^{-3} gauss for energy-selection field intensities of 0.1 gauss. Surveys made of the magnetic field variations existing in the plane of the existing cesium ion-cesium atom cross-section measurements are shown in Figs. 1 to 3 for a region which is typical in size to the one required for the electron-cesium atom measurements. In Fig. 1 a relative measurement of the variation in the vertical component of the background magnetic field is plotted as a function of position. Plotted in Figs. 2 and 3 are the variations in the horizontal components of the background field as a function of position. It should be noted that the background field is composed of contributions from the earth's magnetic field as well as contributions from various electrical sources in the region adjacent to the experiment. As can be seen from the field plots in Figs. 1 to 3, a maximum variation of approximately 17×10^{-3} gauss occurs over the experimental region. In the same region the maximum intensity of the background magnetic field was on the order of 0.6 gauss.

On the basis of the magnetic field surveys, the major problem in achieving desired accuracies is the nonuniformity in the magnetic field that exists in the measurement volume. To eliminate effects of rapid variations in field intensity, a magnetic shield will be positioned outside the vacuum system around the experimental volume. The purpose of the shield is to reduce the magnitude of the variations in the background field intensity. The shield will not, however, be used to completely cancel the entire ambient intensity of the background field. A three-dimensional Helmholtz coil configuration placed outside the shield will be used to cancel the ambient background field over approximately a 4 ft^3 volume. Thus with the external Helmholtz coils used in conjunction with the magnetic shield, the volume within the shield can be made essentially free of significant magnetic field effects. The energy-selection field will be generated by coils placed inside the shield but outside the vacuum system. The shield system is designed so that saturation of the shield due to the magnetic field produced by the energy-selection field occurs at operating field intensities where the 17×10^{-3} gauss variation in the background field is no longer significant. To insure that residual fields do not build up within the shield and other associated parts of the apparatus, the magnetic field intensity within the system will be measured continuously with a three-dimensional Hall-type probe which has been calibrated in a known field to the desired one per cent accuracy at 0.1 gauss.

To insure minimum perturbations from the vacuum tank which houses the experiment, all welds and wall areas are being located a maximum distance from the critical regions of the experiment, and only highly nonmagnetic materials, such as copper and 310 stainless steel, are being used in the critical portions of the system.

Analysis of Electron-Atom Total Collision Cross Sections

A fundamental collisional parameter related to the basic properties of an atom is the differential cross section for elastic scattering, $I(\theta, v)$, which is a function of both scattering angle, θ, and electron velocity, v. In actual physical systems it is the integral of $I(\theta, v)$ over scattering angle that contributes to the over-all observable effect of the particular collisional process under investigation. For example, in the total collision cross-section measurements described in this report, the differential scattering cross section is simply integrated over all angles, since any collision resulting in an angular deflection greater than the angular resolution of the system is counted as a collisional event. With this technique all angular scattering events are weighed equally. The average cross section which is observed experimentally is given by[3]

$$Q_T(v) = 2\pi \int_0^{\pi} I(\theta, v) \sin\theta \, d\theta \tag{2}$$

where Q_T is the total elastic scattering cross section. The 2π factor arises from the fact that the scattering has been assumed isotropic in the plane

perpendicular to the original direction of electron motion so that integration over angle (θ) in this plane can be performed immediately. On the other hand, in many practical applications, such as thermionic energy conversion, the precise change in electron velocity or momentum in a specific direction is the important aspect of a collision. In this case the differential scattering cross section is weighed angularly in order to reflect this effect, and the momentum transfer collision cross section results.

$$Q_M(v) = 2\pi \int_0^{\pi} I(\theta, v)\,(1 - \cos\theta)\sin\theta\, d\theta \tag{3}$$

In Eq. 3 the $(1 - \cos\theta)$ is a weighing factor related to the fractional change of electron velocity or momentum. Clearly this factor has the effect of emphasizing large angle collisions while placing very little emphasis on small angle scattering. For the trivial case where the differential scattering cross section is independent of angle, it can be seen that the total elastic and momentum transfer cross sections are identical. In almost any actual situation the differential cross section will depend on angle, and therefore, it is of interest to estimate the probable difference that will exist between $Q_T(v)$ and $Q_M(v)$.

The angular dependence of electron scattering in a variety of gases was first investigated over thirty years ago by Ramsauer and Kollath.[4] These measurements were made on rare gases, mercury, and several molecular species, for electron energies down to 1.0 eV. The most significant result of this work was the conclusion that the electron scattering has a pronounced angular dependence with distinct maxima and minima exhibited in some cases as a result of quantum effects. Unfortunately, little additional work has been done along this line, and to date no differential scattering data exists for the alkalis or for any atomic species for energies less than 1.0 eV. Nevertheless, the available data can be used to determine a reasonable estimate of the effect that the angular dependence of electron scattering might have on the two averages, Q_T and Q_M. As an illustration, $I(\theta)$ data (summarized in Ref. 5) for neon corresponding to energies between 1.0 and 4.0 eV and for carbon dioxide corresponding to energies between 1.0 and 2.0 eV are shown in Figs. 4 and 5. This data, which is typical of the gases investigated, indicates vividly that electron scattering is definitely dependent on angle and that the angular dependence can change substantially over a small energy range. Using Eqs. 2 and 3, the total elastic and momentum transfer cross sections have been determined from the data of Fig. 4. The results of this numerical calculation are shown in Fig. 6. In the case of neon it is seen that Q_T is always 15 to 25 per cent higher than Q_M over the energy range covered. However, for the lower energies in CO_2, as shown in Fig. 7, large angle scattering dominates, and consequently, Q_M is approximately 20 per cent larger than Q_T. As the energy increases, this trend reverses itself until at approximately 2.0 eV, Q_T is 15 per cent larger than Q_M. Numerical experimentation of this type has also been carried out for a variety of hypothetical $I(\theta, v)$ functions in an attempt to determine the sensitivity of Q_T and Q_M to variations in $I(\theta)$. Of significance is the fact that even though the differential scattering cross section may depend strongly on angle, the integration process (Eqs. 2 and 3) is very effective in minimizing the effect.

After integrating several angular trial functions for $I(\theta, v)$ based on typical trends in available data, it was determined that for the cases treated near 1.0 eV, the difference between Q_T and Q_M was less than 50 per cent.

As has been mentioned, no differential scattering data exists for cesium. In fact, Brode's[1] data represents the only available total electron-atom collision cross-section measurements for cesium in any energy range. The electron-cesium atom momentum transfer cross sections determined in the first year of this contract (Appendix I) from the transport properties of a cesium arc plasma are not in complete agreement with extrapolations of Brode's total electron-atom cross-section measurements. The lack of agreement could occur if Q_T and Q_M differed appreciably for cesium near 1.0 eV. In two recent theoretical calculations[6,7] of the electron scattering cross sections for cesium, the Q_T was found to be 50 to 100 per cent larger than Q_M near 1.0 eV. This result seems to be consistent when compared with data available for other gases, which was described in the previous paragraph. Therefore, even though the total and momentum transfer elastic scattering cross sections for cesium would be expected to have similar qualitative and quantitative behavior in the vicinity of 1.0 eV, preliminary analysis of the available differential scattering data for various gases, the available Q_T and Q_M data for cesium, and the theoretical predictions of Q_T and Q_M for cesium would seem to indicate that a difference in magnitude between Q_T and Q_M would be expected near 1.0 eV and that this difference might be on the order of 50 to 75 per cent.

Outline of Research for the Next Six-Month Period

1. Construction and assembly of the electron-cesium atom beam experiment will be completed.

2. All components of the system will be calibrated. This includes the magnetic field energy-selection system and the neutral cesium pressure measuring system.

3. Measurements will be made of the total electron-cesium atom collision cross section over the energy range from 0.5 to 2.5 eV.

CESIUM ION-CESIUM ATOM COLLISION PROBABILITY MEASUREMENTS

Introduction

In diffusion-dominated plasmas the loss rate of ions from the plasma is determined by their mobility. Accurately predicting the loss rate of ions from the ignited-mode cesium plasma existing in the thermionic converter is one of the important terms required in the calculation of the energy balance equations for the system. In the previous periods cesium ion-cesium atom total collision cross sections were measured over an energy range from 10.0 eV down to energies near 0.1 eV. The results of these investigations were reported at the Fourth International Conference on the Physics of Electronic and Atomic Collisions held in Quebec, Canada, on August 2 through 6, 1965. In these measurements an electroformed collision chamber was employed to eliminate contact potential effects so that the energy of the ion beam could be determined uniquely. Ion beams with energies as low as 0.058 eV were detected successfully with this system. To determine the energy dependence and magnitude of the diffusion cross section required for mobility calculations, the charge exchange cross section was determined from the measured total collision cross-section information by calculating the total contribution of elastic scattering events to the measured total collision cross section. The elastic scattering cross section was calculated on a completely classical basis as outlined in Ref. 2, assuming the potential for the interaction was purely an inverse fourth power dependence or in effect only due to dipole interactions. It has been recently shown experimentally by Menendez and Datz[8] in differential scattering measurements of cesium ions on argon, krypton, and nitrogen that rainbow effects occur at low energies and that it is important to include even at low energies a 4-6-12 type potential of interaction to accurately predict the magnitude of the elastic scattering cross section.

One of the large uncertainties that has existed in the cesium ion-cesium atom cross-section measurements which will also be a problem in the low-energy electron-cesium atom measurements is the determination of true cesium density in the collision chamber. It has been reported by Nolan and Phelps[9] and by Sheldon and Manista[10] that an appreciable length of time is required for the cesium pressure in the system to come into equilibrium once a pressure change is produced by changing the temperature of the cesium reservoir.

Therefore, in this report period a re-examination of cesium pressure determination techniques was made in an effort to eliminate the problems associated with determining an absolute cesium pressure in the scattering chamber, and the effects of including a 4-6-12 potential on the determination of the cesium elastic scattering cross section were evaluated.

Cesium Pressure Determinations

In earlier attempts to determine the time required for a pressure change in the cesium reservoir system to come into equilibrium in the scattering chamber, the change in attenuated ion beam current passing through the collision chamber was measured as a function of time for a fixed cesium reservoir system temperature. In these measurements the temperature of the cesium reservoir was adjusted so that there was sufficient pressure in the collision chamber to produce an attenuation of the ion beam. The variation in ion beam attenuation was then measured as a function of time after a temperature change occurred in the reservoir. Any variation of the ion beam under these conditions was interpreted as being produced by changes in the neutral density of cesium atoms in the collision chamber. By this technique an estimate was obtained of the time required for the pressure in the collision chamber to equilibrate. On the basis of these measurements, it was concluded that the time required for the cesium pressure to equilibrate was short in comparison to the time in which the measurements were obtained.

Observations of this phenomenon made by other investigators, for example, Nolan and Phelps[9] and Sheldon and Manista,[10] indicate that the time for the cesium density to equilibrate is on the order of hours rather than the much shorter time constants inferred on the basis of ion beam attenuation measurements. In an attempt to resolve this difference and also to increase the accuracy of the cross-section measurements, a surface ionization gauge detector has been used to measure the neutral efflux of cesium from a cesium reservoir system which was designed so that the chamber located directly over the reservoir could be maintained at a temperature which was significantly hotter than the temperature of the cesium reservoir. This type of configuration was used in the measurements because it most closely approximated the situation existing in the actual cross-section measurements. The cesium was introduced into the reservoir in a manner in which only pure cesium with no foreign materials, such as glass from the cesium ampule, was present in the reservoir. The surface ionization gauge detector was a 0.006-in. diameter tungsten filament which was outgassed for several days prior to operation to reduce the level of emission of impurity ions from the tungsten surface. In the measurement of the neutral efflux from a 0.040-in. diameter hole located in the upper chamber of the reservoir system, the tungsten filament was operated at approximately 1950°C. Shown in Fig. 8 is a typical ion current variation measured as a function of time for the system. The ion current measured is proportional to the neutral efflux of cesium from the 0.040-in. diameter hole. This efflux should be proportional to the neutral density in the upper chamber of the reservoir. Therefore, by measuring the number of cesium ions produced by contact processes on the tungsten surface, it is possible to determine the relative change in the neutral cesium density in the upper portion of the cesium reservoir system as a function of reservoir temperature and time. As indicated in Fig. 8, the time required to achieve relative temperature stability in the system is on the order of three minutes. Beyond this point approximately one minute is required to achieve stability of the neutral efflux of cesium from the system. Measurements made up to times of thirty minutes indicate, as shown in Fig. 8, that no significant change in neutral efflux

occurs at the detector, which can be interpreted as indicating that no gross change in neutral density occurs in the upper portion of the cesium reservoir. In these measurements the temperature of the reservoir was maintained to within approximately $1^{o}C$. Closer control of the temperature of the reservoir was not possible with the existing heating system. The relatively rapid, small variation of ion current detected as a function of time can be attributed to this effect. The important feature of this data is that the average level of the ion current did not change with time. Cycling the system down to the initial starting reservoir temperature, which was below the ambient temperature of the surrounding walls of the vacuum system, produced results which were more typical of those observed by other investigators. The temperature of the reservoir, as indicated in Fig. 8, required approximately ten minutes to achieve relative stability. In this case, however, the ion current level required an additional nine minutes to achieve stability. In all cases tested, it was found that significantly longer times were required to achieve ion current stability when the reservoir was significantly lower in temperature than the surrounding parts of the system and when significant amounts of cesium had just previously been effused from the reservoir. By carefully monitoring the background ion current level detected in the system at a position that was a significant distance from the hole in the cesium reservoir, it was ascertained that the higher ion currents detected prior to achieving stability when cycling the reservoir from a high temperature to one lower than the surrounding environment were always accompanied by higher background levels. Therefore, a very reasonable explanation of the long time dependence required to achieve equilibrium density conditions which is supported by the background measurements is that significant effects due to cesium adsorbed on the walls of the surrounding system are contributing to the detected ion current level. In both the cesium ion-cesium atom and electron-cesium atom measurements, this effect is eliminated by the liquid nitrogen cold traps which are located in critical regions of the system.

Repeated cycling of the system yielded consistent results in that all pressure levels checked achieved stability in the ion current level in times on the order of one minute, whereas cycling to the low initial reservoir temperature always resulted in significantly longer times to achieve equilibrium. To insure that the longer times required on recycling to the initial reservoir temperature were not truly a hysteresis effect that would be present in all measurements, a series of tests was conducted by first increasing the reservoir temperature and then by reversing the direction of the temperature cycling process. The results of these measurements are shown in Fig. 9. In all cases the time required to achieve stability was on the order of one minute, and excellent agreement was achieved between the measured current levels on the increasing portion of the temperature cycle and the decreasing portion of the cycle.

On the basis of the results obtained in these tests to date, it must be concluded that if precautions are taken to insure that the cesium reservoir system has good high-vacuum qualities and is not subject to attack by cesium and if the effects of wall pumping by the surrounding environment of the reservoir are eliminated by the proper use of liquid nitrogen cold traps, the time required to achieve

an equilibrium neutral cesium density in the collision chamber is on the order of one minute rather than time scales which are significantly longer.

Further measurements using a hot wire detector are presently under way to determine the neutral cesium efflux rates from the exit slit of the actual operating electroformed collision chamber system to insure that the larger volume associated with this system does not significantly alter the time required to achieve neutral cesium density equilibrium within the chamber.

Analysis of Elastic Scattering Cross Sections

In the analysis of the total collision cross-section information, as has been previously outlined,[2] the diffusion cross section used in the mobility calculations was determined by calculating classically the elastic contribution to the measured total collision cross section. By subtracting this elastic contribution from the measured total collision cross section, the charge exchange contribution can be determined. In this analysis, an inverse fourth power interaction potential was assumed to hold for the lower energy scattering interactions under investigation in the ion-atom measurements. The validity of this assumption as a result of the recent measurements reported by Menendez and Datz[8] is subject to considerable question. In the measurements of Menendez and Datz, it was found that a significant rainbowing effect occurred at relatively large scattering angles for cesium ions interacting with argon, krypton, and nitrogen. The presence of this rainbow in the experimental differential scattering cross section implies that the use of an inverse fourth power potential to describe the elastic scattering interaction at these low energies is undoubtedly incorrect. It has been suggested by Mason and Vanderslice[11] that a 4-6-12 type potential should be considered even for exremely low energy interactions, especially when dealing with relatively large particles, such as the cesium system. The general form of the potential used to calculate differential scattering cross sections is given by

$$Q(r) = \frac{\epsilon}{2}\left[(1+\gamma)\left(\frac{r_m}{r}\right)^{12} - 4\gamma\left(\frac{r_m}{r}\right)^{6} - 3(1-\gamma)\left(\frac{r_m}{r}\right)^{4}\right] \tag{4}$$

where

ϵ is the potential well depth.

γ is a strength parameter of the r^{-6} portion of the potential.

r_m is equilibrium internuclear distance.

In Eq. 4 the r^{-4} term includes the charge-dipole and the charge-induced dipole interactions and the r^{-6} term includes charge-quadrupole, charge-induced quadrupole, and induced dipole-induced dipole interactions. The last term in this expression which is the r^{-12} portion of the potential is the short-range repulsion term. When two particles having the potential function of the type described in Eq. 4, in which

there are both attractive and repulsive portions, interact, there is a relative energy region in which rainbow phenomenon will be observed in the angular scattering distribution. This effect will also significantly alter the magnitude of the differential scattering cross section. Calculations have been carried out to determine the differential elastic scattering cross section as a function of energy for the cesium system to see if any significant alteration in the magnitude of the predicted elastic scattering cross section would result from the inclusion of these additional terms in the interaction potential. In these calculations a value of 4.4 Å was used for the equilibrium internuclear distance. This value was obtained from the work of DeBoer[12] on the spectra of the cesium molecular system. A value of $\gamma = 0.5$ and a value of the polarizability of cesium equal to 52.3 $Å^3$ as determined from the measurements of Salop, et al.,[13] were used to determine the value of the well depth, ϵ , from the following expression:

$$3/2(1-\gamma)\epsilon r_m^4 = \frac{e^2\alpha}{2} \tag{5}$$

Shown in Fig. 10 is the differential scattering cross section calculated for a relative interaction energy of 3.38 eV. As can be seen in this figure, there is a significant rainbowing effect observed in the differential scattering cross section at an angle of approximately 1.7 radians in the center-of-mass system. Shown in Fig. 11 is the calculated differential scattering cross section for a relative energy of 0.543 eV. In this case the rainbowing effect is not as readily apparent. However, as in the case of the higher energy calculation, the differential scattering cross section determined from the 4-6-12 interaction potential as a function of angle is significantly larger than that predicted with only an inverse fourth power interaction potential. The over-all contribution of this effect to the predicted elastic scattering cross section results in approximately a 25 per cent increase in the predicted elastic scattering cross-section values in the energy range of the cesium ion-cesium atom cross-section measurements. The magnitude of the cross section predicted using the 4-6-12 type interaction potential is sensitive to the values of r_m, ϵ , and γ used in the calculation. In the results presented, every attempt was made to use the most reliable estimates of these values. On the basis of these results further work is being carried out to determine the limits of uncertainty of the calculation due to the uncertainties associated with the determination of the values of ϵ , r_m, and γ and to evaluate the effect a possible change in the magnitude of the elastic scattering cross section will have on the determination of cesium ion mobilities.

It is interesting to note that the presence of this effect in the cesium ion-cesium atom system can be detected at relatively large scattering angles. Shown in Fig. 12 is the calculated variation in the differential scattering cross section as a function of energy for a center-of-mass scattering angle $\theta = 1.57$ radians. As shown in this figure, a pronounced bump in the differential cross section would occur approximately in the 3.0 to 4.0 eV range if a 4-6-12 interaction potential were applicable for this type of system. Also plotted for comparison in this figure is the differential scattering cross section which would be predicted only for an inverse fourth power potential.

Outline of Research for the Next Six-Month Period

1. Measurements will be made of the cesium efflux rate from the exit slit of the electroformed collision chamber system to determine a true neutral density in the collision chamber as a function of cesium reservoir temperature.

2. On the basis of the density measurements, further cesium ion-cesium atom cross-section measurements will be conducted to firmly establish the velocity dependence of the total cross section at low energies.

3. Calculations of the cesium ion mobility will be carried out using the existing total collision cross-section information with the new 4-6-12 type interaction potential.

REFERENCES

1. R. Brode, Phys. Rev. 34, 673 (1929).

2. R. H. Bullis, "The Measurement of Low-Energy Cesium Ion-Atom Cross Sections by Beam Techniques," presented at the Fourth International Conference on the Physics of Electronic and Atomic Collisions held in Quebec, Canada, on August 2 through 6, 1965.

3. E. W. McDaniel, COLLISION PHENOMENA IN IONIZED GASES, J. Wiley & Sons, New York (1964).

4. C. Ramsauer and R. Kollath, Ann. Physik 12, 527 (1932).

5. S. C. Brown, BASIC DATA OF PLASMA PHYSICS, Tech. Press of M.I.T. and Wiley (1959).

6. P. M. Stone and J. R. Reitz, Phys. Rev. 131, 2101 (1963).

7. J. Crown and A. Russek, Phys. Rev. 138, A665 (1965).

8. M. G. Menendez and S. Datz, "Measurement of the Angular Distribution of Elastically Scattered Cs^+ Ions from Ar, Kr, and N_2," presented at the Fourth International Conference on the Physics of Electronic and Atomic Collisions held in Quebec, Canada, on August 2 through 6, 1965.

9. J. F. Nolan and A. V. Phelps, Bull. Amer. Phys. Soc. 8, 445 (June, 1963).

10. J. Sheldon and E. Manista, private communication.

11. E. A. Mason and J. T. Vanderslice, J. Chem. Phys. 31, 594 (1959).

12. J. H. DeBoer, ELECTRON EMISSION AND ABSORPTION PHENOMENA, Cambridge Press 1935, page 171, reprint University Microfilms, Ann Arbor, Michigan, 1962.

13. A. Salop, E. Pollack, and B. Bederson, Phys. Rev. 128, 2243 (1962).

LIST OF FIGURES

Fig. 1 Background Magnetic Field Vertical Component

Fig. 2 Background Magnetic Field Horizontal West Component

Fig. 3 Background Magnetic Field Horizontal South Component

Fig. 4 Angular Distribution of Electrons Scattered in Neon[5]

Fig. 5 Angular Distribution of Electrons Scattered in Carbon Dioxide[6]

Fig. 6 Calculated Variation Between Q_T and Q_M for Neon

Fig. 7 Calculated Variation Between Q_T and Q_M for Carbon Dioxide

Fig. 8 Time Variation of Cesium Ion Current

Fig. 9 Measured Ion Current Variation with Reservoir Temperature

Fig. 10 Calculated Differential Scattering Cross Section - 3.38 eV

Fig. 11 Calculated Differential Scattering Cross Section - 0.543 eV

Fig. 12 Calculated Differential Scattering - θ = 1.57 Radians

BACKGROUND MAGNETIC FIELD

VARIATION IN INTENSITY IN UNITS OF 10^{-3} GAUSS

VERTICAL COMPONENT

-8	-5	-3	0	2	5	7	7
-8	-5	-2	0	2	5	6	8
-7	-5	-3	0	2	3	5	8
-7	-5	-2	0	2	5	8	9
-5	-3	0	2	5	7	8	9
-5	-3	-1	2	3	5	7	8
-5	-3	0	2	5	6	8	9

← 6 INCHES →

← 7 INCHES →

FIG. 1

FIG. 2

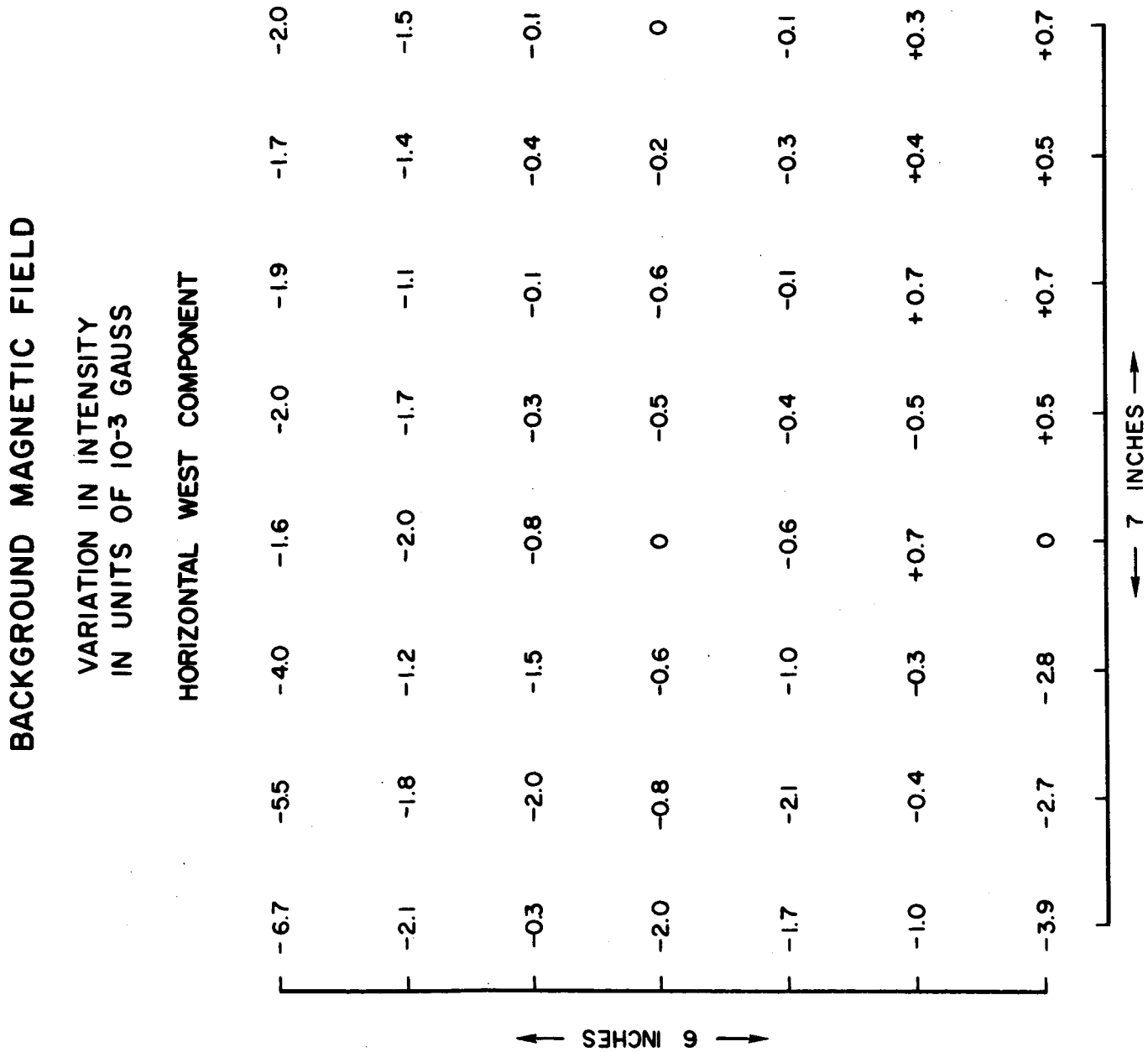
BACKGROUND MAGNETIC FIELD
VARIATION IN INTENSITY
IN UNITS OF 10-3 GAUSS
HORIZONTAL WEST COMPONENT
-6.7 -5.5 -4.0 -1.6 -2.0 -1.9 -1.7 -2.0
-2.1 -1.8 -1.2 -2.0 -1.7 -1.1 -1.4 -1.5
-0.3 -2.0 -1.5 -0.8 -0.3 -0.1 -0.4 -0.1
-2.0 -0.8 -0.6 0 -0.5 -0.6 -0.2 0
-1.7 -2.1 -1.0 -0.6 -0.4 -0.1 -0.3 -0.1
-1.0 -0.4 -0.3 +0.7 -0.5 +0.7 +0.4 +0.3
-3.9 -2.7 -2.8 0 +0.5 +0.7 +0.5 +0.7
6 INCHES
7 INCHES

FIG. 3

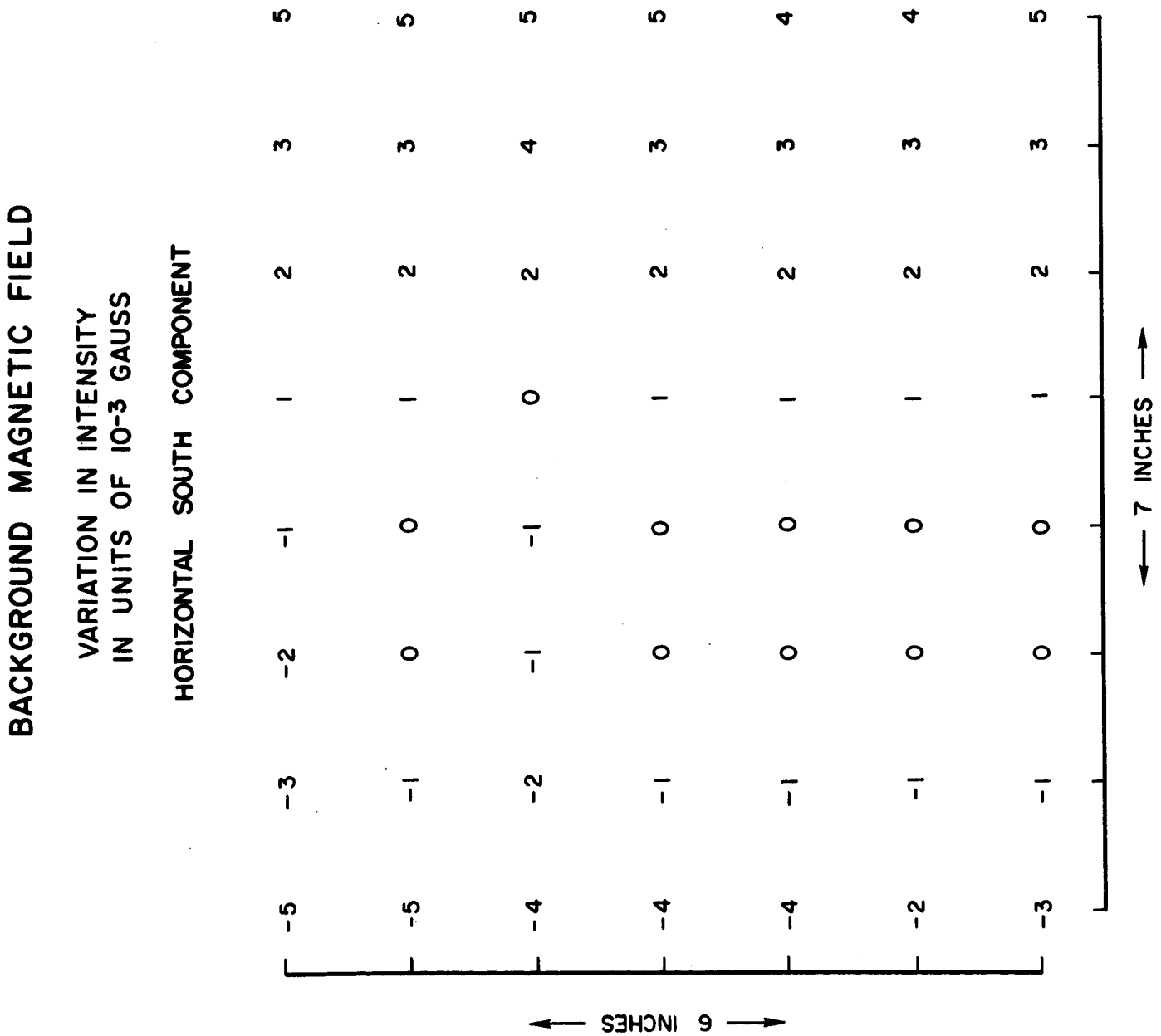
BACKGROUND MAGNETIC FIELD
VARIATION IN INTENSITY
IN UNITS OF 10-3 GAUSS
HORIZONTAL SOUTH COMPONENT
-5 -3 -2 -1 1 2 3 5
-5 -1 0 0 1 2 3 5
-4 -2 -1 -1 0 2 4 5
-4 -1 0 0 1 2 3 5
-4 -1 0 0 1 2 3 4
-2 -1 0 0 1 2 3 4
-3 -1 0 0 1 2 3 5
6 INCHES
7 INCHES

ANGULAR DISTRIBUTION OF ELECTRONS SCATTERED IN NEON (REF. 4)

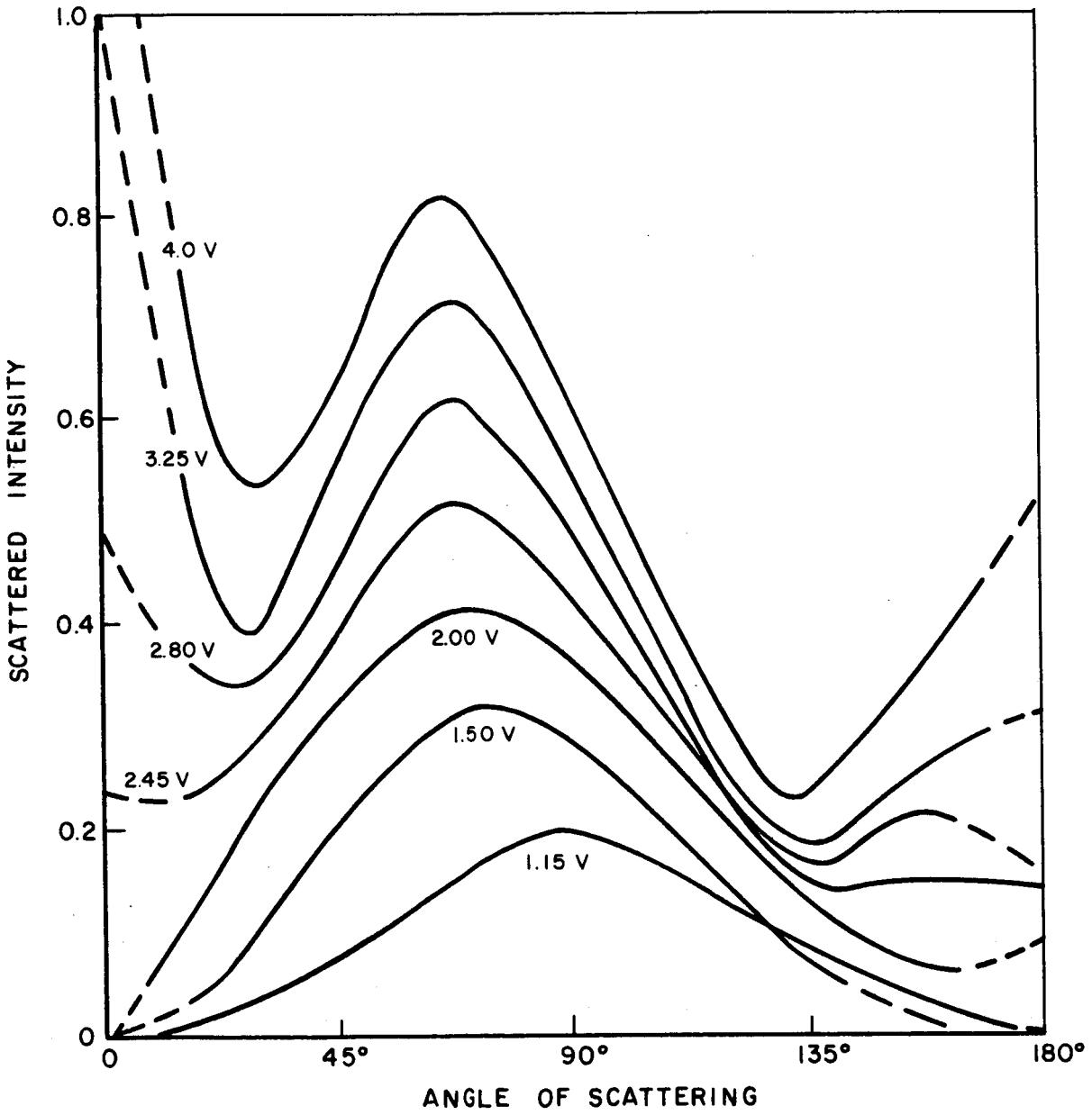

ANGULAR DISTRIBUTION OF ELECTRONS SCATTERED IN CARBON DIOXIDE (REF. 4)

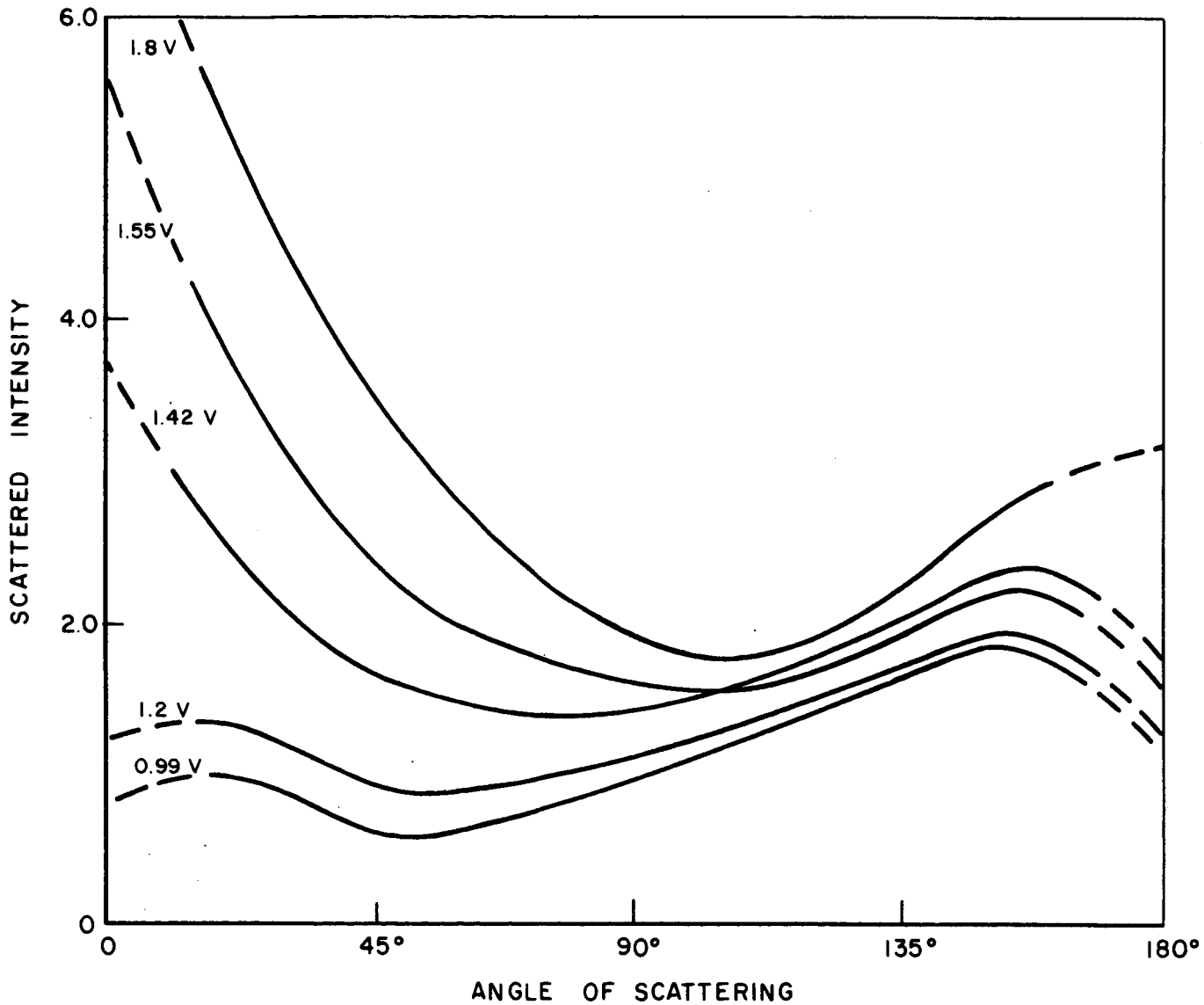

FIG. 6

CALCULATED VARIATION BETWEEN Q_T AND Q_M FOR NEON

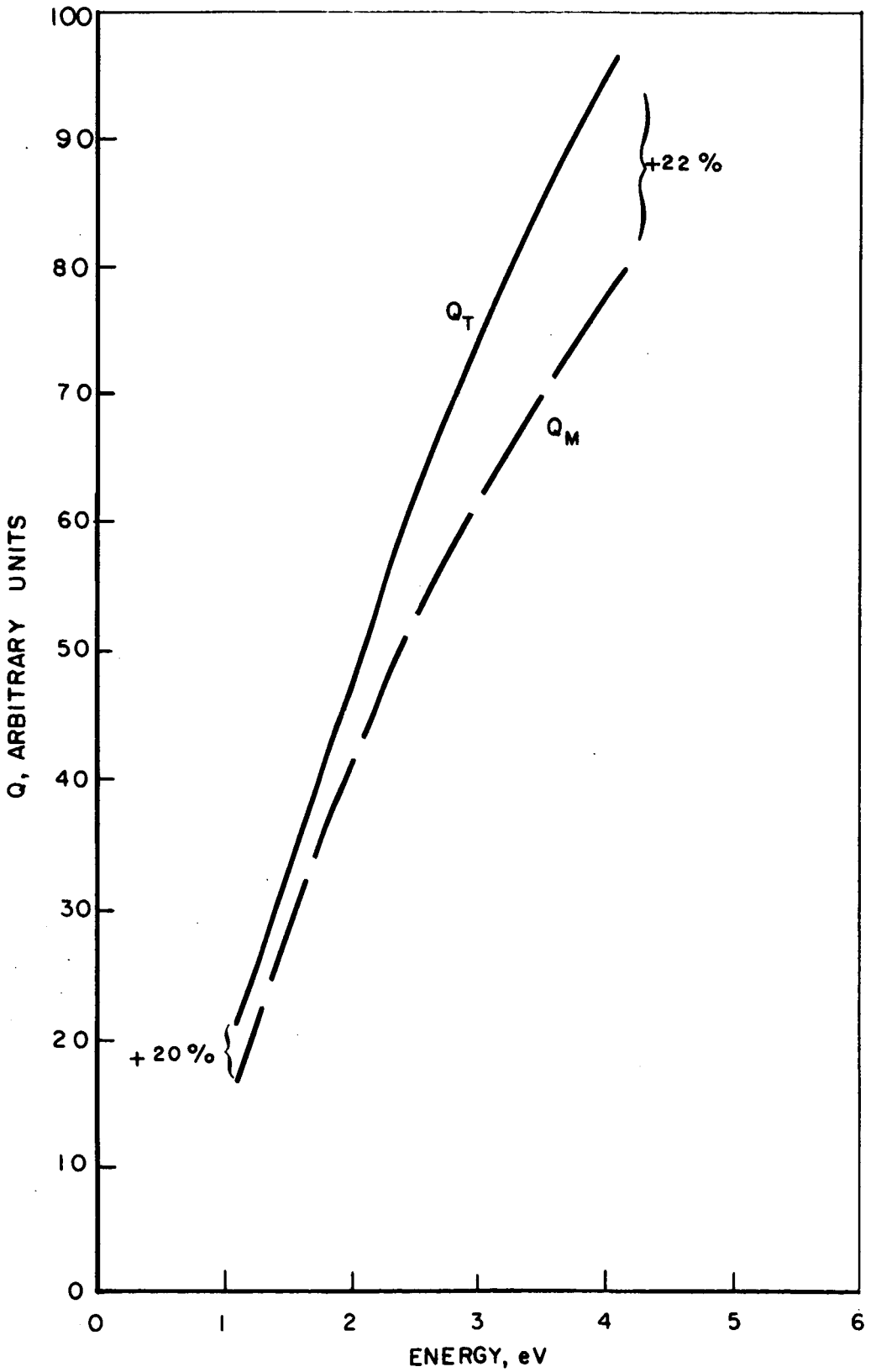

FIG. 7

CALCULATED VARIATION BETWEEN Q_T AND Q_M FOR CO_2

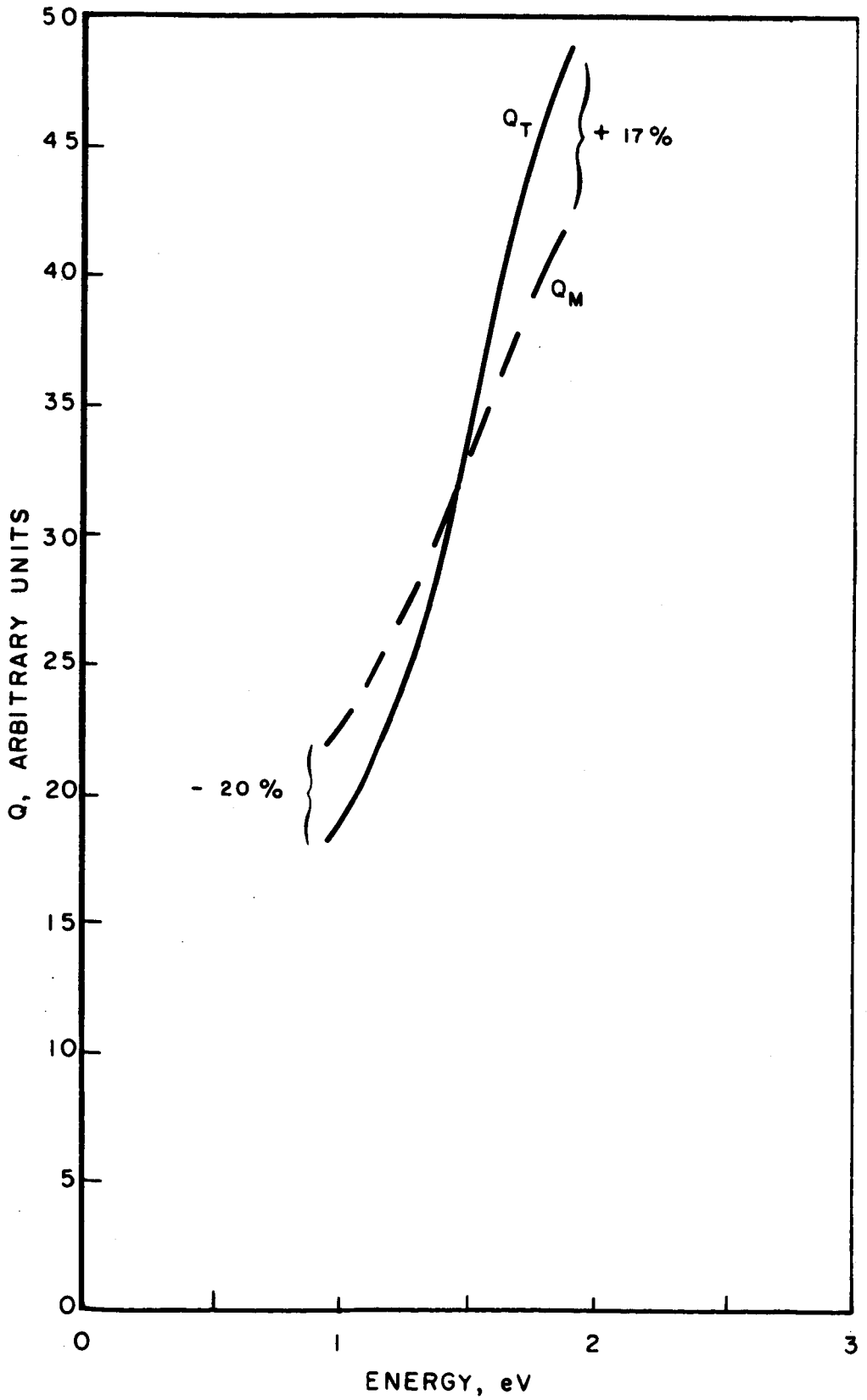

FIG. 8

TIME VARIATION OF CESIUM ION CURRENT

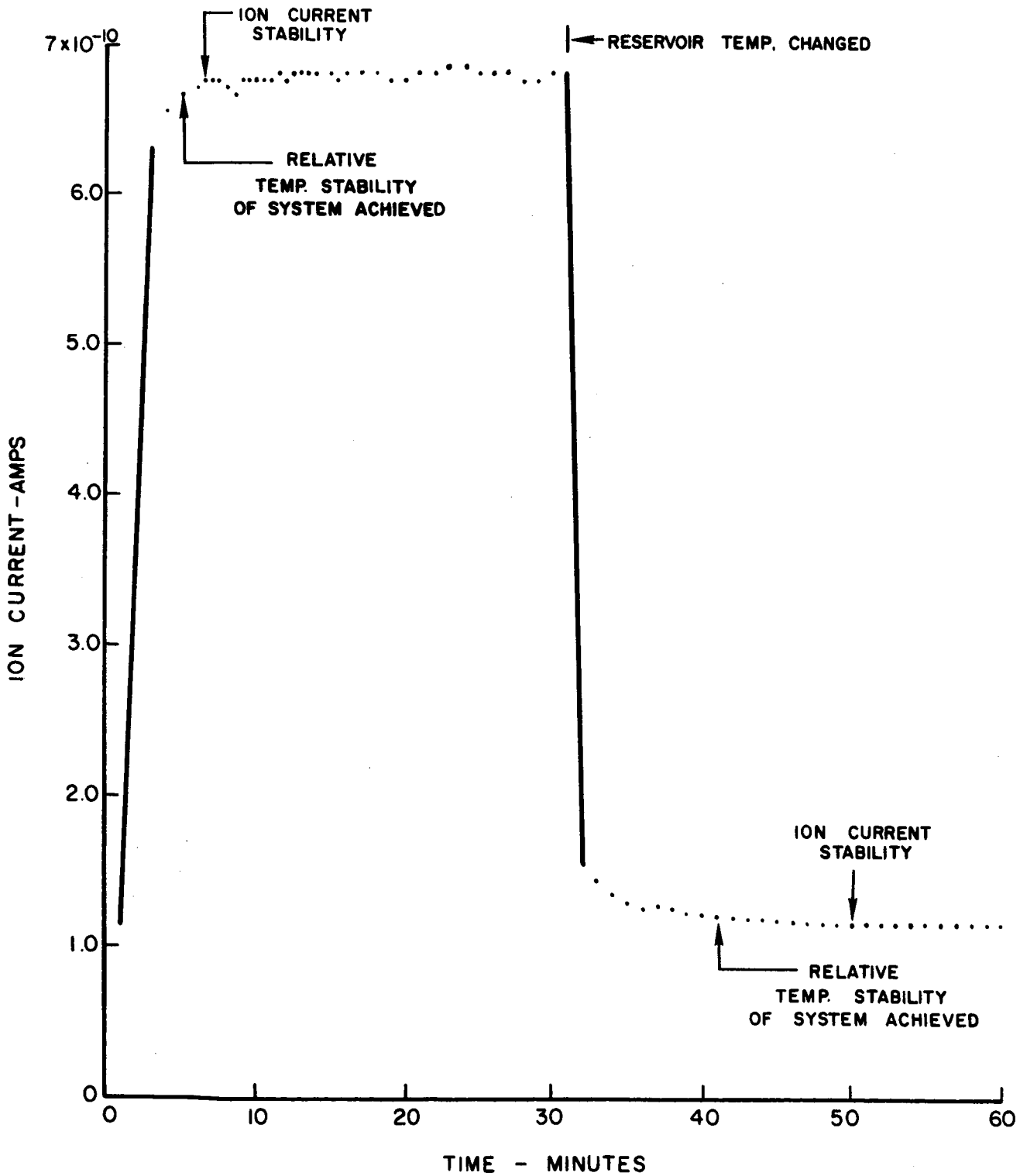

FIG. 9

MEASURED ION CURRENT VARIATION WITH RESERVOIR TEMPERATURE

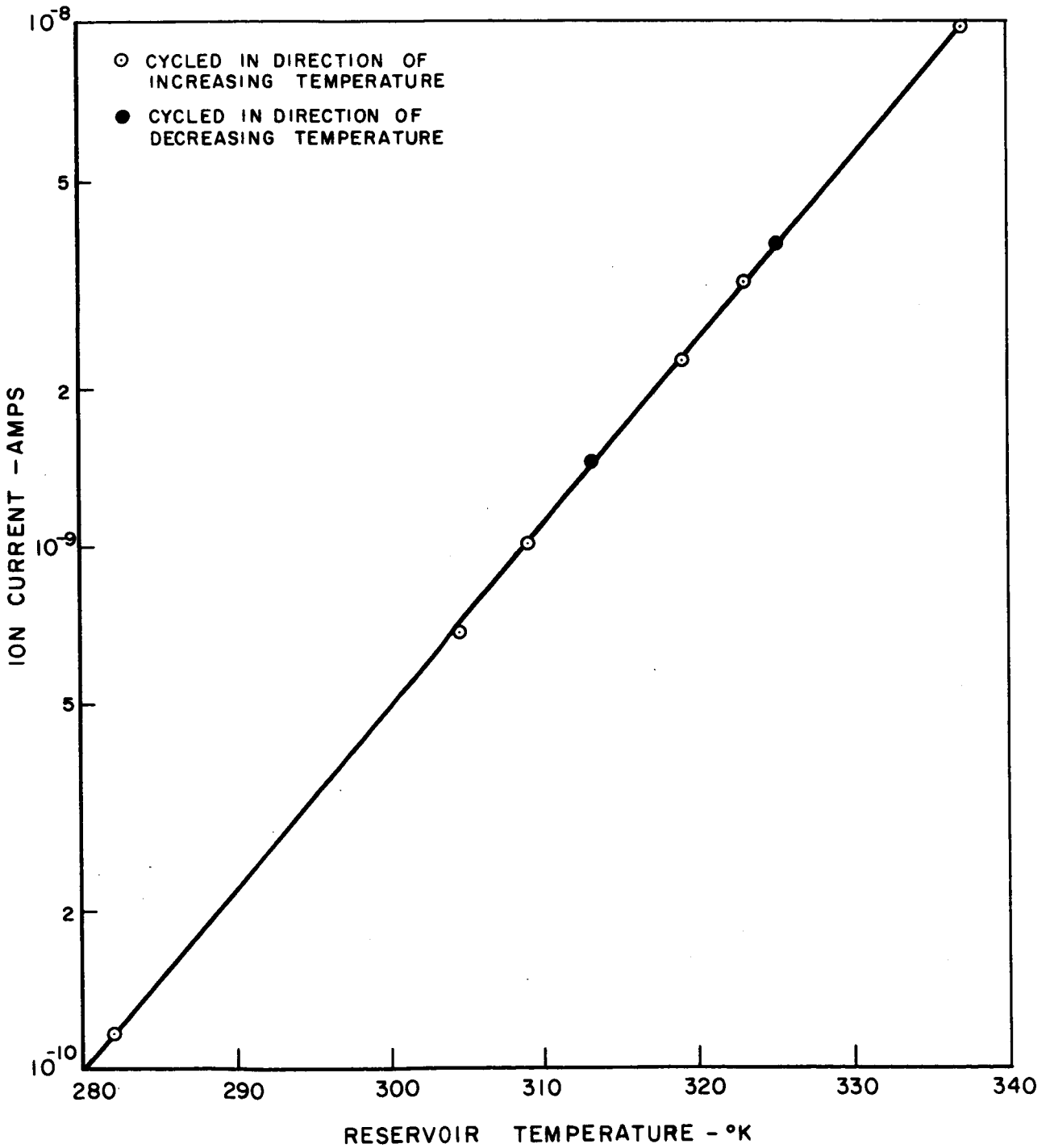

CALCULATED DIFFERENTIAL SCATTERING CROSS SECTION

3.38 eV

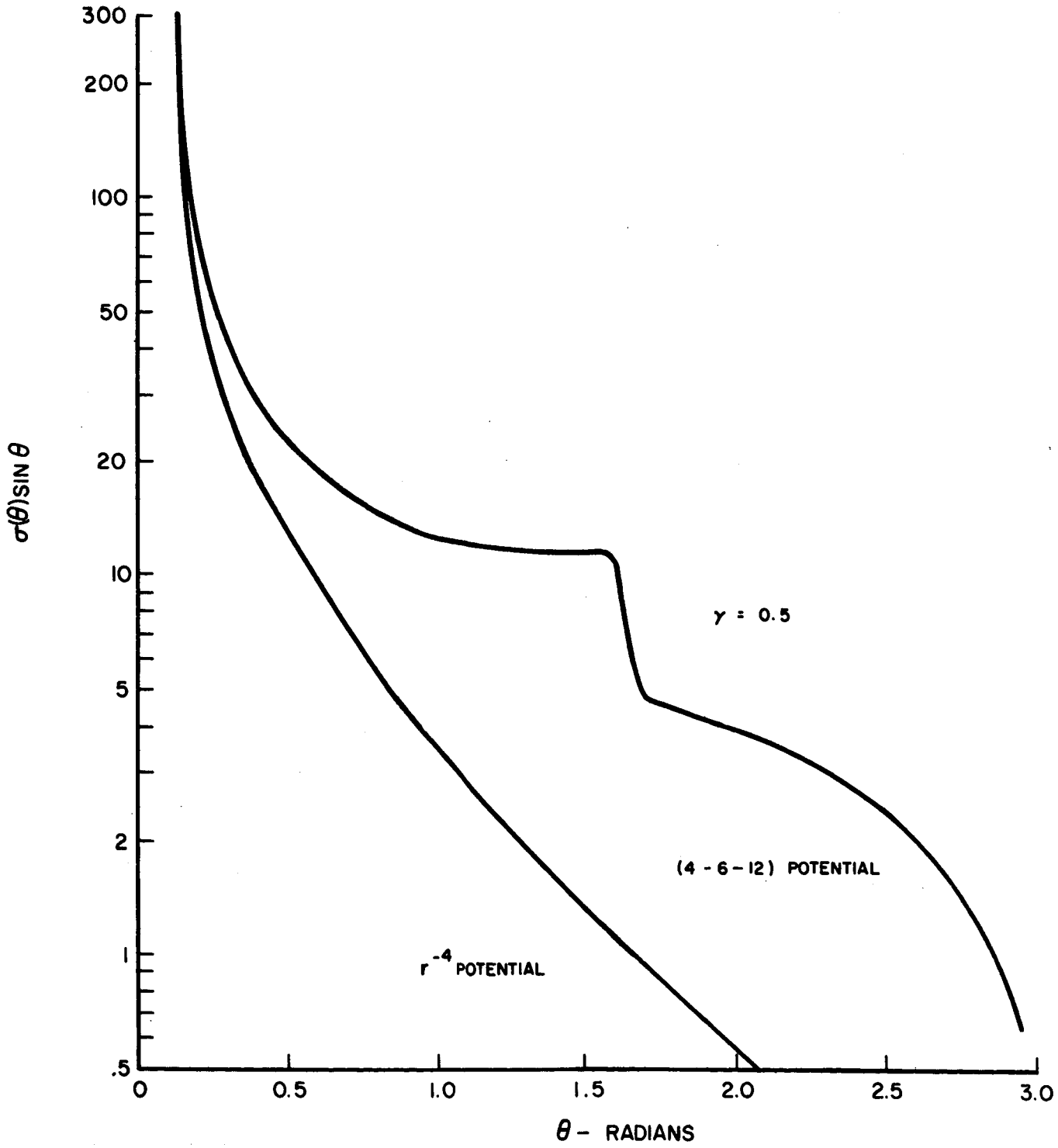

CALCULATED DIFFERENTIAL SCATTERING CROSS SECTION
0.543 eV

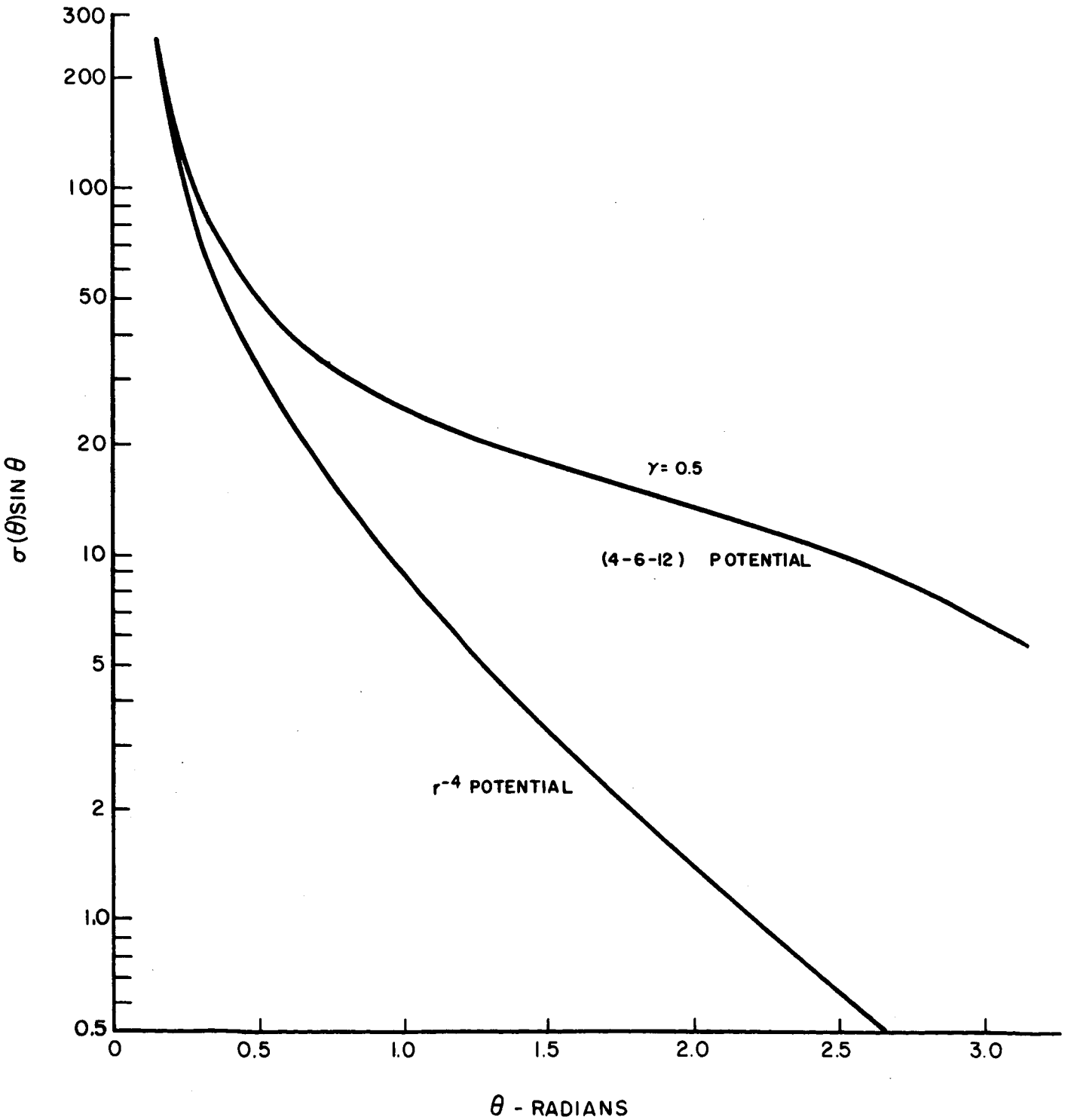

CALCULATED DIFFERENTIAL SCATTERING

θ = 1.57 RADIANS

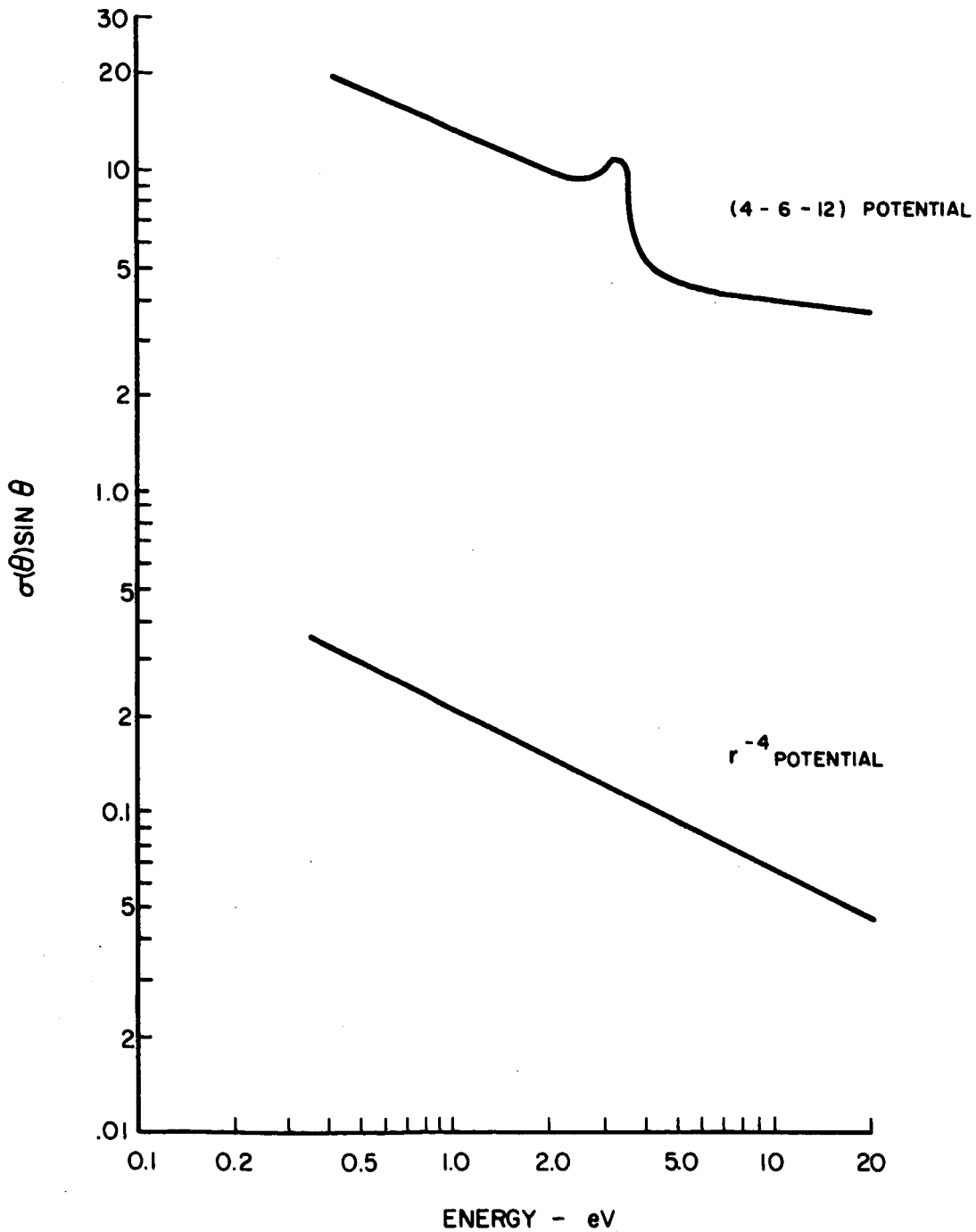

D-920243-18

APPENDIX I

LOW-ENERGY ELECTRON-CESIUM ATOM COLLISION PROBABILITY INVESTIGATIONS

By

W. L. Nighan
United Aircraft Research Laboratories, East Hartford, Connecticut

Presented at the
Fourth International Conference on the Physics
of Electronic and Atomic Collisions
Quebec, Canada
August 2-6, 1965

D-920243-18

LOW-ENERGY ELECTRON-CESIUM ATOM COLLISION PROBABILITY INVESTIGATIONS*

William L. Nighan
United Aircraft Research Laboratories, East Hartford, Connecticut

Abstract

The elastic electron-cesium atom momentum transfer collision probability has been determined in the electron velocity range corresponding to 0.45 to 0.80 $\sqrt{eV}$. The collision probability was determined from an analysis of an effective electron-heavy particle collision frequency obtained from measurements of the plasma properties in a cesium arc discharge. The effective collision frequency was found to be strongly dependent on electron temperature in the 2000 to 5000°K range and significantly dependent on plasma degree of ionization for values of this parameter greater than 10^{-4}. The collision probability determined from an analysis of the integral equation describing the effective collision frequency has been found to be a strong function of electron velocity having a pronounced minimum of approximately 100 to 300 collisions per cm mm Hg in the 0.45 to 0.65 $\sqrt{eV}$ range of electron velocities, rising to a value about an order of magnitude larger in the velocity range corresponding to 0.75 to 1.0 $\sqrt{eV}$.

1. Introduction

Electron-atom momentum transfer collisions are known to play a dominant role in the determination of the transport properties of slightly and partially ionized plasmas. As a result, a knowledge of the elastic electron-cesium atom collision cross section for momentum transfer, i.e., collision probability, is a prerequisite for obtaining an understanding of the physical properties of the non-equilibrium plasma that exists in thermionic converters and other plasma devices employing cesium vapor in an ionized state. In most practical cesium plasma devices, electron mean energies are less than 1.0 eV. In this range of electron energies there is approximately an order of magnitude variation in the experimental cross-section values reported in the literature with no particular energy dependence exhibited in the data.

A compilation of the available electron-cesium atom collision probability data is presented in Fig. 1. R. B. Brode[1] measured the total collision probability (approximately equal to the momentum transfer collision probability for nearly isotropic scattering) over thirty years ago using monoenergetic electron beam techniques. His measurements cover a range down to an electron energy of approximately 0.6 eV and are considered to have established at least the approximate magnitude and general qualitative behavior of the collision probability for energies near 1.0 eV. However, experimental difficulties associated with the use of very low-energy electron beams have prevented the extension of these methods to lower energies, and in fact, Brode's measurements have not even been checked for cesium at the higher energies. The data presented in Refs. 2 through 11 have been determined from electron swarm experiments where the electrons are distributed in velocity over almost the entire energy range from 0 to 1.0 eV. These experiments were each designed to measure a different

*Portions of this work were supported by the National Aeronautics and Space Administration under Contract NAS3-4171.

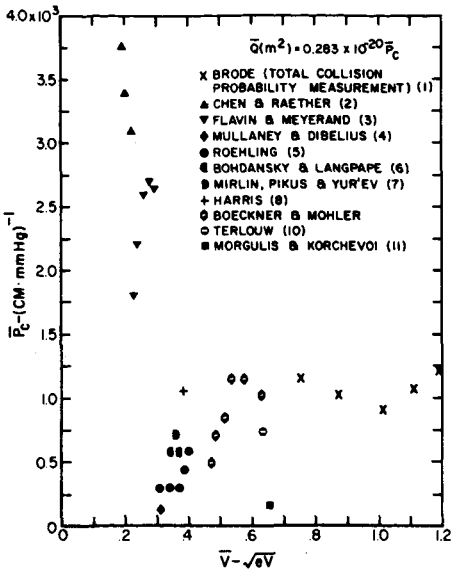

Fig. 1 Available Electron-Cesium Atom Collision Probability Data

electron transport property in a cesium plasma from which an average collision probability was then determined. Unfortunately, the importance of proper averaging of the velocity-dependent collision probability over electron velocities has not been appreciated, and since plasma transport properties depend on the averaging process, large discrepancies in the various measurements can exist as a result of misinterpretation of experimental data, even though the measurements may be substantially correct.

Another significant point concerns the contribution made by electron-ion collisions in the various investigations. For approximately half of the available experimental collision probability data, particularly those obtained from device studies, electron-ion effects have been neglected altogether. For the other half it has been assumed that electron-atom and electron-ion resistive effects can be treated separately and added like resistivities without regard to the method of averaging over the electron velocity distribution. This procedure and other such averaging techniques can result in large errors in the interpretation of experimental data if the collision probability is a strong function of electron velocity, as most of the available experimental and theoretical work for cesium indicates.

The objective of the research program reported herein was to obtain experimental data from measurements of the plasma properties in the positive column of a dc cesium arc discharge, which is amenable to analytical and laboratory diagnosis. These measurements lead to an effective electron-cesium heavy particle collision frequency from which the actual momentum transfer collision probability is then obtained from an analysis of the integral transport equation describing the effective collision frequency. With these results a comparison is made with the existing collision probability data interpreted on a common basis and with the available theoretical predictions of the electron-cesium atom collision probability.

2. Theory and the Plasma Model

The equation describing the electron current flow through a plasma under the influence of a dc electric field may be derived on the basis of the physical model for

a plasma originally developed by Lorentz.[12, 13, 14] In this approach it is assumed that collisions are instrumental in setting up a nearly spherically symmetric velocity distribution of electrons and that small deviations from spherical symmetry are described with sufficient accuracy by the second term in the spherical harmonic expansion of the velocity distribution function. Upon substitution of this first order expansion into the Boltzmann equation, two coupled equations describing the relationship of the terms of the expansion result. From these relations and the equation for particle current, the following equation may be obtained for the current density J:

$$J = -\frac{4\pi}{3}\frac{n_e e^2}{m}\int_0^\infty \frac{v^3(\partial f_0/\partial v)}{\nu_{ea}(v)+\nu_{ei}(v)}\, dv\, E\,, \qquad \text{(I-1)}$$

where m, e, v, and n_e are the electron mass, charge, velocity, and number density, E the electric field intensity, f_o the isotropic part (first term in the spherical harmonic expansion) of the electron velocity distribution function normalized with respect to electron density, and $\nu_{ea(i)}$ the elastic electron-atom (ion) collision frequency for momentum transfer. The velocity-dependent electron-atom and electron-ion collision frequencies are related to their respective momentum transfer cross sections by

$$\nu_{ea}(v) = n_a Q_{ea}(v)v \qquad \text{and} \qquad \nu_{ei}(v) = n_i Q_{ei}(v)v, \qquad \text{(I-2)}$$

where n_a is the atom number density, $Q_{ea}(v)$ the elastic electron-atom momentum transfer cross section, n_i the ion number density (equal to the electron number density in a neutral plasma) and $Q_{ei}(v)$ is the effective elastic electron-ion momentum transfer cross section. In the derivation of Eq. 1 it has been assumed that the plasma is homogeneous, that the collisional friction force exerted on electrons is due to elastic momentum transfer encounters with heavy particles which are assumed infinitely massive in comparison with electrons, and that electron-electron encounters have no direct influence on the momentum of the electron gas. A more complete analysis of the problem, which yields this result, is presented in Ref. 13.

For the cesium arc discharge plasma (to be described in Section 2), which is the subject of this analysis, the relatively high degree of ionization ($>10^{-4}$) results in extremely short electron thermalization times. Therefore, it will be assumed that electron-electron collisions are instrumental in establishing a Maxwellian distribution of electron velocities. Using the Maxwellian form for the electron velocity distribution and Eq. 2 relating collision frequency to cross section results in the following expression for the current density:

$$J = \frac{8}{3\sqrt{\pi}}\frac{\alpha e^2}{m}\left(\frac{m}{2kT_e}\right)^{\frac{5}{2}}\int_0^\infty \frac{v^3 e^{-\frac{mv^2}{2kT_e}}}{Q_{ea}(v)+\alpha Q_{ei}(v)}\, dv E \qquad \text{(I-3)}$$

where k is Boltzmann's constant, T_e the electron temperature, and α the degree of ionization defined as the ratio of electron density to atom density.

Equation 2 relates the elastic electron-ion momentum transfer collision frequency to an effective electron-ion collision cross section which represents the

collective effects of electron-ion interactions. Isolated coulomb collisions in a plasma cannot be physically distinguished because of the long range of the coulomb force field. However, as an approximation a two-body coulomb collision term can be derived classically in which scattering is limited to particles within a Debye sphere about the test charge. This procedure eliminates the divergence of the integral describing the effective electron-ion momentum transfer cross section and reasonably accounts for the shielding effect which results in the necessarily finite value for the cross section. The derivation of the effective electron-ion collision term presented in detail in Refs. 13 and 15 reduces to the following expression:

$$Q_{ei}(v) = \frac{e^4}{4\pi\epsilon_0^2 m^2 v^4} \cdot \log_e \left[\frac{12\pi(\epsilon_0 kTe/e^2)^{3/2}}{n_e^{1/2}}\right] \tag{I-4}$$

where ϵ_0 is the permittivity of free space. The representation of the effect of electron-ion interactions by Eq. 4 is adequate for the purpose of this investigation, since electron-ion effects never dominate in the range of plasma conditions encountered in this experiment.

In the analytical development leading up to Eq. 3, it was assumed that the plasma was homogeneous. In the case of the cylindrical cesium arc discharge, it is assumed that axial and circumferential uniformity exists and that the only gradient in the radial direction is the electron density variation resulting from particle diffusion to the walls of the discharge tube. Because there are no significant plasma gradients in the direction of discharge current flow, the plasma behaves as though it were homogeneous, and a simple averaging process can be used to account for the radial variation in discharge current density caused by the diffusion gradient in electron density. Since it is assumed that circumferential uniformity in plasma properties exists, the current flow through a cross-sectional area of the discharge tube is given by

$$I = 2\pi \int_0^R J(r)\, r\, dr\ , \tag{I-5}$$

where I is the discharge current and R the tube radius. If it is assumed that the radial variation in degree of ionization can be reasonably represented by a parabola of the form

$$\alpha(r) = \alpha_0(1-r^2/R^2), \tag{I-6}$$

where α_0 is the degree of ionization on the tube axis (n_{e_0}/n_a), and this form is then used in conjunction with Eq. 3, Eq. 5 becomes

$$I = \frac{16\sqrt{\pi}}{3} \cdot \frac{\alpha_0 e^2}{m}\left(\frac{m}{2kT_e}\right)^{\frac{5}{2}} \int_0^R \int_0^\infty \frac{(1-r^2/R^2)\, v^3 e^{-\frac{mv^2}{2kT_e}}}{Q_{ea}(v)+\alpha_0(1-r^2/R^2)Q_{ei}(v)}\, r\, dv\, dr\, E. \tag{I-7}$$

Since r and v are independent, the radial integration can be performed, and Eq. 7

reduces to

$$I = \frac{16}{3\sqrt{\pi}} \cdot \frac{\alpha_0 e^2}{m} \left(\frac{m}{2kT_e}\right)^{\frac{5}{2}} \int_0^\infty \frac{v^3 e^{-\frac{mv^2}{2kT_e}}}{\alpha_0 Q_{ei}(v)} \left[1 + \frac{Q_{ea}(v)}{\alpha_0 Q_{ei}(v)} \log_e \left(\frac{Q_{ea}(v)}{Q_{ea}(v) + \alpha_0 Q_{ei}(v)}\right)\right] dv \, \frac{\pi R^2}{2} E . \quad \text{(I-8)}$$

It is convenient to define an effective collision frequency from the relationship between current flow and electric field intensity, i.e.,

$$I \equiv \frac{n_{e_0} e^2}{m \nu_{eff}} \cdot \frac{\pi R^2}{2} E . \quad \text{(I-9)}$$

Solving for the effective collision frequency defined by Eqs. 8 and 9 and normalizing with respect to atom density yields

$$\nu_{eff}^{*-1} = \frac{16}{3\sqrt{\pi}} \left(\frac{m}{2kT_e}\right)^{\frac{5}{2}} \int_0^\infty \frac{v^3 e^{-\frac{mv^2}{2kT_e}}}{\alpha_0 Q_{ei}(v)} \left[1 + \frac{Q_{ea}(v)}{\alpha_0 Q_{ei}(v)} \log_e \left(\frac{Q_{ea}(v)}{Q_{ea}(v) + \alpha_0 Q_{ei}(v)}\right)\right] dv = g(T_e, \alpha_0) . \quad \text{(I-10)}$$

Equation 10, defining the normalized effective collision frequency, represents an average of the total normalized electron heavy particle momentum transfer collision frequency and is a function of electron temperature and degree of ionization alone. It should be noted that this normalized effective collision frequency is not the simple average of collision frequency over the velocity distribution but rather is an average of the reciprocal sum of momentum transfer collision frequencies representing specifically the over-all resistive effect of momentum transfer collisions on dc current flow. Spatial averaging has been performed to account for the radial dependence of the electron-ion contribution to the over-all resistance to discharge current flow.

It is apparent from Eq. 10 that a knowledge of the normalized effective collision frequency dependence on electron temperature and degree of ionization could lead to information pertaining to the fundamental electron-atom cross section which appears in the integrand of the integral. An extensive numerical analysis of trial functions for the electron-atom cross section has been carried out based on the experimental information obtained from this investigation. The results of that analysis are presented in Section 5.

The normalized effective collision frequency of Eq. 10 can be related to the measurable parameters of the cesium arc discharge plasma from Eq. 9. Using the perfect gas relationship

$$n_a = \frac{P}{kT_g} , \quad \text{(I-11)}$$

where P and T_g are the cesium vapor pressure and temperature, the following expression for the effective collision frequency is obtained:

$$\nu_{eff}^* = \frac{e^2 k}{2m} \cdot \frac{\pi R^2 n_{e_0} E}{(P/T_g) I} . \quad \text{(I-12)}$$

Equation 12 was used to determine experimentally the normalized effective collision frequency from measurements of electron density, electric field intensity, gas pressure and temperature, and discharge current.

3. Description of the Experiment and Diagnostic Techniques

The theoretical analysis presented in the previous section was used to describe the plasma of the positive column of the cesium arc discharge. The cesium arc discharge was chosen as the laboratory plasma of this investigation because it has properties in the ranges of practical interest and is amenable to analytical and laboratory diagnosis. Of the parameters in Eq. 12 required to obtain experimentally the normalized effective collision frequency, the electron density and temperature are the two most difficult to measure. Various plasma diagnostic techniques are available; however, the most practical for obtaining these particular plasma properties is the electrostatic probe. From an analysis of the current-voltage characteristics of an electrostatic probe, the electron temperature and density can be determined, and the assumption regarding the equilibrium distribution of electron energies verified. In addition, the electric field can be determined from plasma potential measurements made with probes positioned axially along the positive column. A high degree of spatial resolution can be realized with electrostatic probes, and they can be moved from point to point in the plasma to measure local conditions.

An illustration of a typical discharge tube is shown in Fig. 2. Cathode-to-anode separation in this tube was 50 cm and the inside diameter 3.8 cm. During operation the tube was located within a dual oven which controlled the gas temperature and prevented cesium from condensing on the tube walls. The cesium appendix shown in the figure extended down to the lower portion of the oven, which was always held at a lower temperature than the main oven and controlled the cesium vapor pressure. The cesium pressure was determined from the cesium vapor pressure curve of Ref. 16.

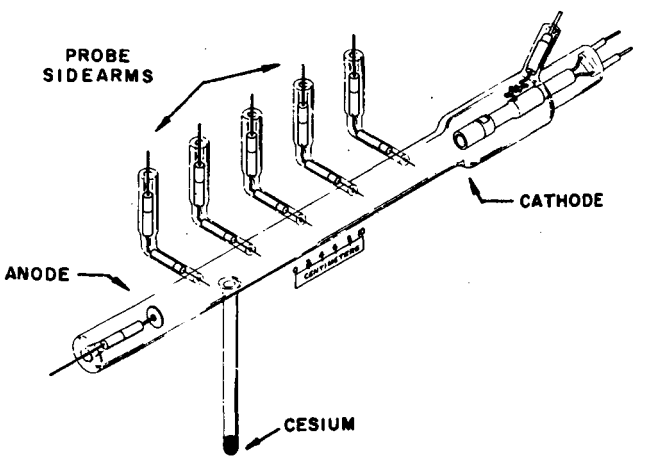

Fig. 2 Cesium Discharge Tube

The electrostatic probe sidearm assemblies were constructed in such a way that the probes, which protruded through a small hole in the wall of the discharge tube, could be moved radially into the plasma by means of a magnet. The probes were constructed of 0.010-in. diameter tungsten rod covered with a glass sheath which served

as an electrical insulator. The entire assembly averaging 0.018 in. in diameter was ground flat, exposing only the 0.010-in. tungsten tip to the plasma. Great care was exercised in the fabrication of the electrostatic probes in order to make them as small as possible so that the tip of the probe (collection area) exposed to the plasma was both flat and flush with the glass insulation. The probe tips were periodically examined with a microscope at operating temperature in the discharge tube so that any flaw could be detected. A schematic of the movable probe and sidearm assembly is shown in Fig. 3.

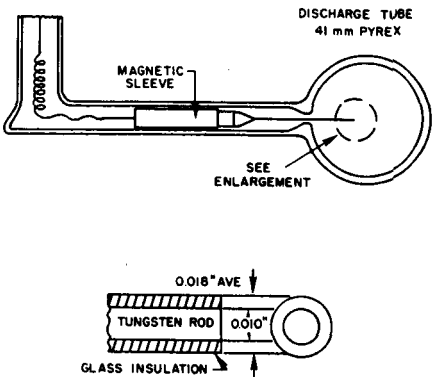

Fig. 3 Movable Electrostatic Probe Sidearm Assembly

The electron temperature, electron density, and plasma potential variations in the discharge have been measured using pulsed electrostatic probe techniques. A pulsing system was used to apply a cleaning pulse, sweep voltage or data acquisition pulse, and rest voltage to the probe; the time duration of each portion of the probe pulse could be varied independently. The time scale of the total pulse applied to the probe with this system ranged from approximately 100 microseconds to 100 milliseconds. With such versatility the effect of changing probe surface conditions, errors due to circuit and plasma response limitations, and the effect of plasma drift or instability can be detected. The importance of being able to vary sweep speed and applied voltage in this manner is detailed in Refs. 17 and 18. A schematic of the pulse waveform is shown in Fig. 4 along with a typical photograph and semilog plot of a probe current-voltage characteristic. The linear behavior of the semilog plots of the electrostatic probe current-voltage characteristic was experimental verification of the existence of a Maxwellian distribution of velocities at least for the slow moving electrons in the body of the distribution which are responsible for the transport properties in the plasma. Deviations from linearity at the low probe currents (approximately 10 microamps) were random in nature and due to the limits of sensitivity of the system.

The approximation of the radial variation of the degree of ionization by a parabola was verified experimentally with the movable electrostatic probes. Radial measurements of electron density have been made over all ranges of discharge current and pressure. A typical plot of the radial density profile is shown in Fig. 5 for various arc currents, where a comparison is made with both the lowest order Bessel function and the assumed parabolic form. It is apparent from this figure that the assumption of a parabolic radial dependence for the electron density and consequently

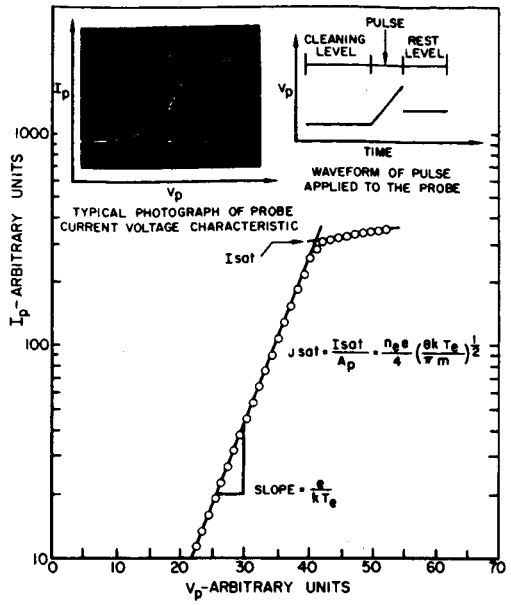

Fig. 4 Typical Semilog Plot of Probe Current-Voltage Characteristic

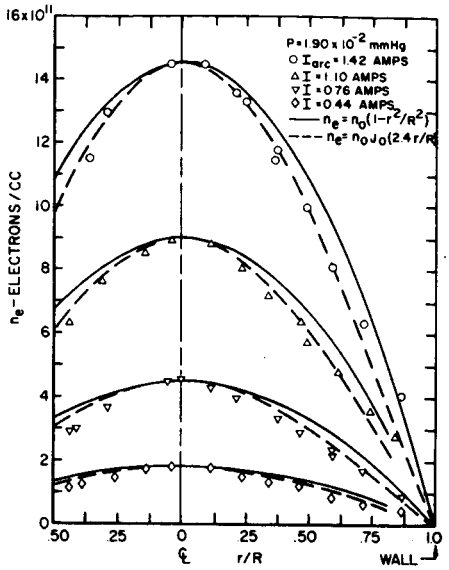

Fig. 5 Variation of Electron Density with Radial Position

the degree of ionization is satisfactory. The electron temperature determined from the radial probe measurements showed no significant dependence on radial position. The axial uniformity of plasma properties was verified from measurements made with electrostatic probes positioned axially along the discharge column. Measurements made over all discharge conditions indicate no significant axial gradients in plasma properties.

Since the physical presence of a probe may significantly perturb a plasma,[19] errors in the determination of electron density from probe measurements can be related to probe size. In order to check on possible perturbations of the plasma resulting from the presence of the electrostatic probes, a special discharge tube was constructed which contained probes of a significantly larger size than the 0.010-in. diameter probes described previously. Incorporated in this tube were three 0.010-in. diameter and two 0.0315-in. diameter electrostatic probes alternately positioned along the tube axis. The large probes occupied a volume about three times as large as the small probes and had a collection area approximately ten times larger. Measurements made over the entire range of cesium pressures, and arc currents used in this investigation indicated no significant variation of either electron density or temperature with probe size. The greatest discrepancy in the electron density, as determined with the large and small probes, was 20 per cent at the highest pressure. On the basis of these results it was concluded that the small 0.010-in. diameter probes did not perturb the plasma for the conditions encountered in this experiment.

4. Measurements and Results

Typical measurements were conducted with cesium pressure and discharge current as independent experimental variables. For moderate cesium pressures

(10^{-2} to 10^{-1} mm Hg) and arc currents (0.3 to 1.5 amps), the electron temperature determined from the slope of the semilog current-voltage characteristics of the electrostatic probes varied from approximately 2500 to 4500°K. From measurements of the plasma floating potential obtained with probes positioned along the axis of the tube and from a knowledge of the spacing between probes, the electric field intensity was determined and found to vary from about 0.2 to 0.6 volts/cm. The electron density on the axis of the tube varied from approximately 10^{11} to 3×10^{12} electrons/cc. From these values of the electron density and the cesium atom density calculated from the perfect gas law (Eq. 11), the degree of ionization along the tube axis, α_0, was obtained. Because of the radial variation of electron density and the independence of atom density on tube radius, the degree of ionization varied radially in the same manner as the electron density (Fig. 5).

Using the relationship of Eq. 12, the normalized effective electron-cesium heavy particle collision frequency has been determined over the range of plasma variables from the experimental data of several test runs. Figure 6 presents this effective collision frequency as a function of electron temperature and degree of ionization on the tube axis. The effective collision frequency data of this

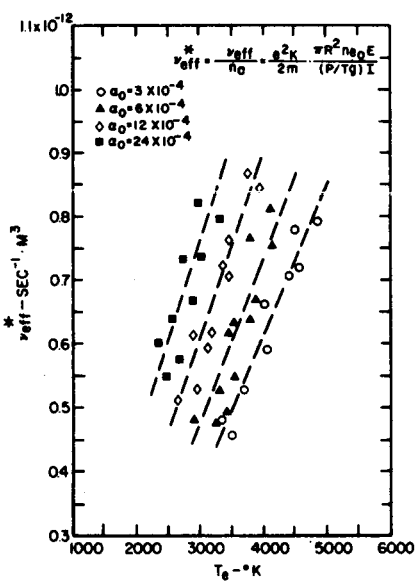

Fig. 6 Experimentally Determined Normalized Effective Electron-Cesium Heavy Particle Collision Frequency

figure were obtained from two different discharge tubes and several electrostatic probes positioned at different points along the tube axis. In spite of this variation in experimental conditions, the scatter in the data points was very small. As is apparent from Fig. 6, a clearly defined trend in the collision frequency exists with both electron temperature and degree of ionization. Of particular significance is the strong dependence of effective collision frequency on electron temperature. Moving along a constant degree of ionization line, the effective collision frequency increases by a factor of two over the experimental electron temperature range. Also significant is the fact that the collision frequency shows a pronounced dependence on the degree of ionization in the 10^{-4} to 10^{-3} range, where electron-ion effects in cesium plasmas are often neglected. Consequently, the necessity of including electron-ion effects in the theoretical analysis of the plasma model becomes apparent.

5. Analysis of Trial Functions for the Cross Section

Since the experimental measurement of plasma properties leads to a normalized effective electron-cesium heavy particle collision frequency which is an average over all electron velocities, it is necessary to determine how the integral (Eq. 10) describing this collision frequency behaves as a function of electron temperature and degree of ionization for variations in the form of the velocity dependence of the collision probability. Numerical integration techniques permit the analysis of this integrated behavior for a variety of trial forms for the collision probability velocity dependence. Initially, various trial forms were selected on the basis of best estimates as to the magnitude of the collision probability and on trends observed in experimental and theoretical data. Subsequently, hundreds of additional functions representing almost every reasonable magnitude and velocity dependence in the range of interest were numerically integrated, yielding a variety of hypothetical normalized effective collision frequency curves with electron temperature and degree of ionization as variables. This was done so that an accurate estimate of the resolution of the technique could be made and so that trends in the experimental data could be understood and related to the type of cross-section behavior likely to have produced them. Following this procedure a particular class of functions for the velocity-dependent electron-cesium atom momentum transfer cross section has been found, which when integrated, gives the best fit to the experimental data of Fig. 6. The integrated value of this best estimate for the cross section is compared in Fig. 7 with the experimental data. The dashed lines of this figure are

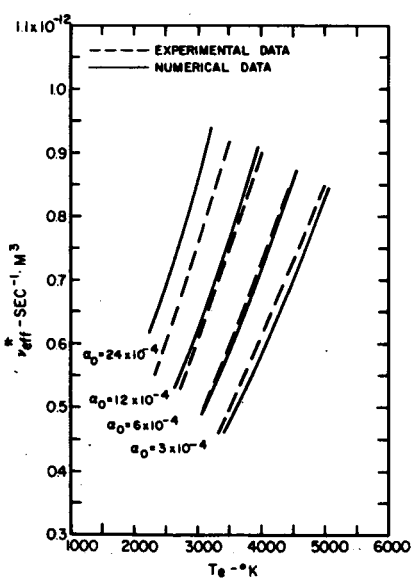

Fig. 7 Comparison of Experimentally Determined and Numerically Calculated Effective Collision Frequency

the same straight lines drawn through the effective collision frequency data of Fig. 6. It is apparent from this figure that the quantitative and qualitative agreement between theory and experiment is quite good. The slope of the effective collision frequency temperature dependence is exactly duplicated by the numerically calculated curve, and the agreement between the two sets of curves for the parametric dependence on the degree of ionization is also very good. The maximum discrepancy that does occur for the highest degree of ionization is only 15 per cent and is well within the limits of

uncertainty of the experiment, the theoretical model, and the theoretical form used to represent electron-ion effects. Therefore, additional refinement of the approximation for $Q_{ea}(v)$ would not be meaningful.

Only one class of functions for the velocity-dependent collision probability yields the agreement between theory and experiment described in the previous paragraph. Figure 8 presents this collision probability as a function of electron velocity. As can be seen from the figure, the collision probability resulting in the best agreement between theory and experiment (solid line in Fig. 8) is a strong function of electron velocity, rising from a minimum value of approximately 100 collisions per cm mm Hg in an electron velocity range corresponding to 0.4 to 0.6 $\sqrt{eV}$ to a maximum over an order of magnitude larger at a velocity in the 0.7 to 0.8 $\sqrt{eV}$ range, where the possibility of a resonance in the collision probability appears to exist. It is this very rapid

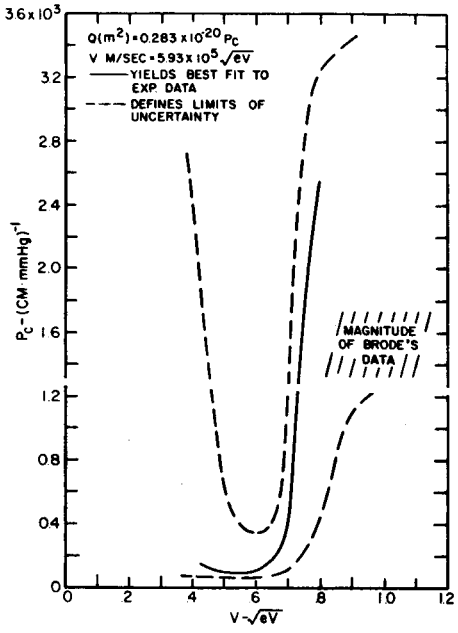

Fig. 8 Electron-Cesium Atom Momentum Transfer Collision Probability

increase in the collision probability at approximately 0.7 $\sqrt{eV}$ that produces the strong electron temperature dependence of the effective collision frequency. There is a loss of sensitivity below approximately 0.4 $\sqrt{eV}$ due to the fact that for lower electron velocities electron-ion interactions begin to dominate the collisional process for the degrees of ionization covered in this experiment. A decrease in sensitivity at the high-energy end of the velocity spectrum results from the small number of electrons in the tail of the electron velocity distribution. However, for higher electron velocities the collision probability must maintain the approximate magnitude indicated by the cross-hatched area of the figure; this magnitude is in agreement with that established by Brode's total collision probability data.[1] Although the collision probability velocity structure cannot be precisely determined above a velocity of approximately 0.8 $\sqrt{eV}$, the magnitude of the collision probability above this level still carries weight in the integration leading to the effective collision frequency. The envelope defined by the dashed lines in Fig. 8 indicates the limits of uncertainty in the collision probability in various velocity ranges; the manner in which the envelope was established is discussed in subsequent paragraphs.

Numerical procedures have been used to establish the degree of uncertainty in the velocity structure of the collision probability resulting from variations in the theoretical expression for the effective collision frequency (Eq. 10) and the effective electron-ion cross section term (Eq. 4); the over-all resolution of the "trial function" technique for the range of experimental variables covered in this investigation has also been considered. The fact that the experimentally determined normalized effective collision frequency is a function of two variables (electron temperature and degree of ionization), rather than the usual single parameter (electron temperature), has been found to result in a significant improvement in the ability of the trial function technique to determine the velocity structure of the collision probability. Numerical experimentation with various trial functions has illustrated the fact that the coupling between the experimental electron temperature range of this investigation and the electron velocity range of sensitivity is substantially strengthened by the normalized effective collision frequency dependence on degree of ionization. This dependence places additional requirements on the exact collision probability velocity structure required to satisfy the experimental effective collision frequency data. In addition, various experimental checks (outlined in Section 3) were made to insure that the plasma diagnostic systems were reliable. Therefore, it is felt that the quantitative and qualitative behavior of the experimentally determined effective collision frequency data and the interpretation of this data resulting in the collision probability of Fig. 8 are correct. However, the possibility always exists that an undetectable systematic experimental error may result in an alteration in the slope but not the magnitude of the effective collision frequency. If this were the case, the absolute magnitude of ν_{eff}^* would not be significantly affected. However, the exact velocity structure of the collision probability as determined from the integral analysis has been found to be quite sensitive to this type of qualitative variation in ν_{eff}^*, particularly at the extremes of the velocity range of interest where the resolution of the technique begins to fade. Therefore, in consideration of such a possibility, a variation of approximately 25 to 50 per cent in the slope of the effective collision frequency data of Fig. 6, equivalent to a variation of about 15 to 20 per cent in the experimentally determined magnitude of ν_{eff}^*, has been taken into account when establishing the envelope of uncertainty for the collision probability velocity structure (dashed lines in Fig. 8). Such a variation is considered reasonable in view of the known limits of accuracy of the experimental techniques.

A family of collision probability curves which forms this envelope has been determined from an analysis of trial functions for $Q_{ea}(v)$. Each member of this family when averaged over all electron velocities yields a normalized effective collision frequency having the quantitative and general qualitative behavior of the ν_{eff}^* data of Fig. 6, subject to the possibility of experimental error as described in the previous paragraph. All the functions defining the envelope have the same qualitative behavior as the collision probability curve yielding the best fit to the experimental data of this investigation. However, it is apparent from the figure that the total increment of uncertainty (ΔP_c) in the collision probability magnitude as defined by the envelope can be quite large, particularly at the extremes of the velocity range of sensitivity. This should not be interpreted as meaning that any collision probability curve falling within the envelope will, when averaged, satisfy the experimental data of this investigation. For example, an increase in the magnitude of the collision probability in the lower velocity range of sensitivity (0.4 to $0.5\sqrt{eV}$) must be accompanied by an appropriate decrease at higher velocities such as to yield the same

magnitude and approximately the same slope as the ν_{eff}^{*} data of Fig. 6 when averaged over the electron velocity distribution. It should be noted that the collision probability of Fig. 8 is not experimental data but rather is based on the interpretation of experimental data. The range of uncertainty in the precise velocity structure of the collision probability, as determined from the analysis described above, is a reasonable indication of the possible variations associated with this interpretation and also indicates the importance of consistent and realistic interpretation of "average" or "effective" collision probability data determined from experimental measurements of over-all collisional effects in plasmas.

6. Discussion of Results

The necessity of including electron-ion effects in the analysis of cesium plasmas in the ranges of electron temperature and degrees of ionization of practical interest, and the importance of proper averaging of the electron-cesium heavy particle collision probabilities over electron velocities have prompted a re-evaluation of the available average cesium collision probability data reported in the literature. Of the available cesium collision probability data (Fig. 1), only in Refs. 2 and 3 has an attempt been made to determine the actual velocity dependent collision probability from an integral analysis. References 4 through 11, involving measurement of a variety of plasma transport properties, inferred an average collision probability from an effective collisional term defined to represent the over-all effect of collisions on the particular transport property under investigation. This average collision probability was then plotted as a function of most probable or average electron velocity determined from a measurement of electron temperature. In addition to normal experimental error, the collision probability determined in this manner is subject to the uncertainties associated with differences in the averaging of the cross section over electron velocities which is complicated by the influence of electron ion interactions. In Refs. 5, 9, and 10 an attempt to account for the effect of electron-ion collisions was made, and it was assumed that electron-atom and electron-ion effects could be treated separately and added like resistivities. However, this approach is not satisfying physically and in fact can result in large errors in the interpretation of the velocity structure of the collision probability when $Q_{ea}(v)$ is a strong function of electron velocity and comparable in magnitude to $\alpha Q_{ei}(v)$. Consequently, the data of Fig. 1 represents only the approximate magnitude of the collision probability in the electron velocity range of interest. An improvement in the understanding of the cesium collision probability data results if the available data is converted to an effective collision frequency form and plotted as a function of electron temperature. This is accomplished by converting the velocity coordinate of each data point of Fig. 1 to the electron temperature corresponding to the most probable velocity of a Maxwellian distribution. A normalized effective collision frequency is recovered by multiplying each collision probability data point by its corresponding most probable velocity point. This conversion process results in a presentation of the available experimental data in a form more closely associated with the manner in which the measurements were actually made and provides a base for a reasonable comparison with the data of this investigation.

Figure 9 presents the available experimental data[2 - 11] in effective collision frequency form, the data of this investigation, and the numerically calculated normalized effective collision frequency extrapolated to lower and higher electron

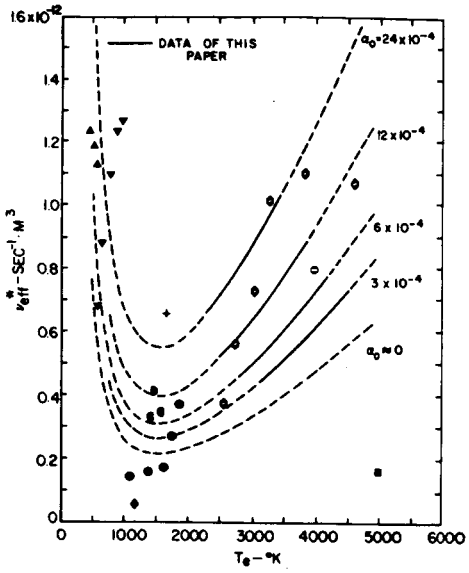

Fig. 9 Numerically Calculated Normalized Effective Collision Frequency Compared with Available Data in Effective Collision Frequency Form

temperatures. Although the lowest electron temperature of the current investigation was approximately 2500°K, the integrated collision probability (effective collision frequency) can be numerically calculated for lower electron temperatures with reasonable safety, since at lower temperatures and degrees of ionization in the 10^{-4} to 10^{-3} range, electron-ion effects begin to dominate the collisional processes. The numerical curves in Fig. 9 were obtained using Eq. 10 and the collision probability of Fig. 8 (solid line) which has been extrapolated smoothly to lower and higher electron velocities in accordance with the magnitudes established by Refs. 2 and 3 in the 0.1 to 0.3 $\sqrt{eV}$ range and with the magnitude of Brode's data in the 1.0 $\sqrt{eV}$ range. Even though the electron velocity distribution function would be non-Maxwellian for very low degrees of ionization, ν^*_{eff} has also been calculated neglecting electron-ion effects ($\alpha \approx 0$ in Fig. 9) in order to illustrate the fact that for a degree of ionization of approximately 10^{-4} electron-ion effects first become significant in the 2000 to 5000°K range of electron temperatures. Examination of Fig. 9 indicates that interpretation of the available cesium collision probability information on the basis of an effective collision frequency formulation including the effect of electron-ion collisions produces a definable trend in the data. Of particular significance is the agreement between the numerical and experimental data establishing the magnitude of the minimum of ν^*_{eff} in the 1000 to 2000°K range. The minimum value of ν^*_{eff} is determined by the minimum in the collision probability velocity structure, i.e. Fig. 8. When interpreting Fig. 9, it should be noted that the information presented in Refs. 2 - 11 does not permit calculation of ν^*_{eff} in exactly the same form for each case and no attempt has been made to replace electron-ion effects that have been removed.[5, 9, 10] Therefore, in comparing the numerically calculated curves with the available data, emphasis should be placed on the trend established by the data taken as a group rather than on individual values of ν^*_{eff}. The general agreement that results when the available data are analyzed on a more common basis and compared with the numerically calculated effective collision frequency lends support to the conclusion that the collision probability has a minimum in the 0.5 to 0.8 $\sqrt{eV}$ range of electron velocities as indicated in Fig. 8.

Although even approximate theoretical calculations leading to the electron-cesium atom cross section are quite complicated, current interest has been stimulated

by the practical application of ionized cesium vapor in devices, such as the thermionic converter. It is of interest to analyze some of the more recent theoretical results in light of the conclusions drawn from the experimental and analytical work of this program. The total and momentum transfer electron-cesium atom cross sections were calculated theoretically in Ref. 20. The resultant scattering curves for both the total and the momentum transfer cases are similar with the theoretical curves exhibiting a resonance behavior in the energy range from 0 to 1.0 eV. A more recent calculation[21] of both the total and momentum transfer elastic scattering cross sections has resulted in an extremely sharp resonance in both cross sections at about $0.5\sqrt{eV}$. Of interest is the fact that the total and momentum transfer collision probabilities of Ref. 21 differ by as much as 100 per cent in the 0.7 to $1.0\sqrt{eV}$ range, which would indicate a significant angular dependence of the differential scattering cross section. The theoretical calculations of Refs. 20 and 21 are presented in Fig. 10 along with the collision probability determined from the experimental and numerical data of this program. It is apparent both from the differences in the various theoretical curves

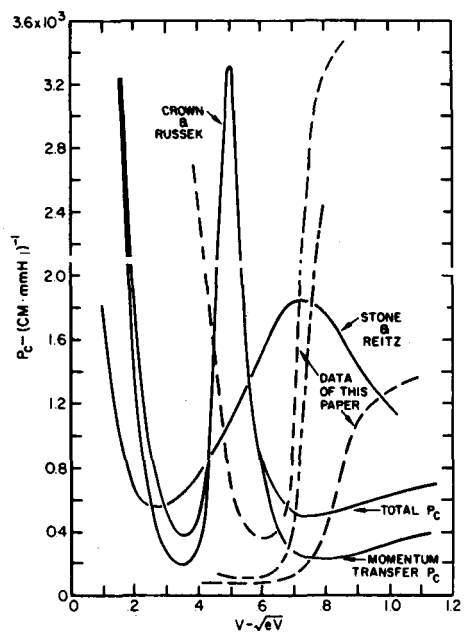

Fig. 10 Theoretically Calculated Collision Probability Compared with the Collision Probability Data of this Investigation

and from examples treated in the original references that the calculated collision probability is extremely sensitive to the theoretical form used to represent polarization effects. However, the general form of the theoretical scattering curves is the same and is in qualitative and semiquantitative agreement with the collision probability data determined in this investigation. Of particular significance is the theoretical prediction of a resonance in the 0.5 to $1.0\sqrt{eV}$ range coupled with a sharp drop to a minimum in the collision probability in the 0.3 to $0.7\sqrt{eV}$ range of electron velocities. In Ref. 21, which is the most recent work and presumably an improvement over previous calculations, an average value of the polarizability was used which corresponds approximately to the average of the experimental values. However, numerical experimentation in Ref. 21 indicates considerable sensitivity to the exact choice of the polarizability. Although the general shape of the theoretical curve remains the same for slight variations in the polarizability, the location of the resonance can be shifted along the velocity scale. Since the

range of maximum sensitivity of this investigation and the data of Refs. 4 through 11 corresponds to the velocity range where theory predicts a sharp dip in the collision probability, the analysis of the numerical and experimental data presented here indicates that the actual location of the collision probability minimum is in the 0.5 to $0.8\sqrt{eV}$ range of electron velocities with the indicated resonance occurring in the vicinity of $1.0\sqrt{eV}$.

7. Conclusions

An analysis has been made of the effective electron-cesium heavy particle momentum transfer collision frequency which was determined from measurements of the plasma properties in a cesium arc discharge. The effective collision frequency has been found to be strongly dependent on electron temperature in the 2000 to 5000°K range and to be significantly dependent on plasma degree of ionization for values of this parameter greater than 10^{-4}. Consequently, the effect of electron-ion collisions must be considered in the analysis of cesium plasmas in the ranges of electron temperature and degrees of ionization of practical scientific and engineering interest.

A numerical analysis of the integral equation describing the effective collision frequency has been conducted in order to determine the sensitivity of the collision frequency to variations in the velocity dependence of the electron-cesium atom momentum transfer collision probability. Numerical experimentation with a wide variety of trial functions for the collision probability has indicated that the resultant effective collision frequency is reasonably sensitive to changes in the velocity structure of the collision probability over the range of experimental variables covered in this investigation. Therefore, it has been possible to determine the general quantitative and qualitative behavior of this velocity dependence over an appreciable range of electron velocities. The collision probability has been found to have a minimum value of approximately 100 to 300 collisions per cm mm Hg in the 0.5 to $0.8\sqrt{eV}$ range of electron velocities, rising to a value about an order of magnitude larger in the 0.75 to $1.0\sqrt{eV}$ range.

Comparison of the effective electron-cesium heavy particle collision frequency determined from this investigation with the available average collision probability data interpreted on the basis of an effective collision frequency formulation including electron-ion interactions, produces a clearly definable trend in the data over a reasonably broad range of electron temperature and degree of ionization. A comparison has also been made between some of the more recent theoretical calculations of the electron-cesium atom collision probability and the experimental and analytical results of this program. Although such calculations are very sensitive to the theoretical form used to represent atomic polarization effects, the resonance behavior of the predicted scattering curves is in quantitative and qualitative agreement with the collision probability velocity dependence determined in this investigation.

Acknowledgements

The author gratefully acknowledges the assistance of Dr. J. H. Bennett of UARL in conjunction with the analysis of trial functions for the electron-cesium atom collision probability. The resourcefullness of Mr. A. H. Witherell in the procurement and construction of experimental facilities is also acknowledged.

REFERENCES

1. R. Brode, Phys. Rev. 34, 673 (1929).

2. C. L. Chen and M. Raether, Phys. Rev. 128, 2679 (1962).

3. R. K. Flavin and R. G. Meyerand, Jr., Proceedings of the IEEE Thermionic Conversion Specialist Conference, Gatlinburg, Tennessee (1963).

4. G. L. Mullaney and N. R. Dibelius, ARS Journal 1575 (November, 1961).

5. D. Roehling, Symposium on Thermionic Power Conversion, Colorado Springs, Colorado, (May, 1962).

6. J. Bohdansky and R. Langpape, Sixth International Conference on Ionization Phenomena in Gases, Paris, Vol. IV, 543 (1963).

7. D. N. Mirlin, G. E. Pikus, and V. G. Yur'ev, Sov. Phys.-Tech. Phys. 7, 559 (1962).

8. L. P. Harris, J. Appl. Phys. 34, 2958 (1963).

9. C. Boeckner and F. L. Mohler, BSJR 10, 357 (1933).

10. J. C. Terlouw, personal communication.

11. N. D. Morgulis, and Yu. P. Korchevoi, Zhurnal Technicichesfoi Fizifi 32, 900 (1962).

12. H. Margenau, Phys. Rev. 69, 508 (1946).

13. H. Dreicer, Phys. Rev. 117, 343 (1960).

14. D. H. Sampson and J. Enoch, Phys. of Fluids 6, 28 (1963).

15. D. J. Rose and M. Clark, Jr., "Plasmas and Controlled Fusion" published jointly by the M.I.T. Press and J. Wiley and Sons (1961), Chapter 8.

16. J. B. Taylor and I. Langmuir, Phys. Rev. 51, 753 (1937).

17. J. F. Waymouth, J. Appl. Phys. 30, 1404 (1959).

18. R. H. Bullis and W. J. Wiegand, Proceedings of the Twenty-third Annual Conference on Physical Electronics at M.I.T. (1963).

19. J. F. Waymouth, Phys. of Fluids 7, 1843 (1964).

20. P. M. Stone and J. R. Reitz, Phys. Rev. 131, 2101 (1963).

21. J. C. Crown and A. Russek, Phys. Rev. 138, A669 (1965).

DISTRIBUTION LIST FOR UNITED AIRCRAFT CORPORATION
Contract No. NAS3-4171
Semiannual and Final Reports

	No. of Copies
Aerojet General Nucleonics San Ramon, California Attention: K. Johnson	1
Aerospace Corporation El Segundo, California Attention: Librarian	1
Air Force Cambridge Research Center (CRZAP) L. G. Hanscom Field Bedford, Massachusetts	1
Air Force Special Weapons Center Kirtland Air Force Base Albuquerque, New Mexico Attention: Chief, Nuclear Power Division	1
Air Force Systems Command Aeronautical Systems Division Flight Accessories Laboratory Wright-Patterson AFB, Ohio Attention: AFAPL (APIP-2, A. E. Wallis)	1
Allison Division General Motors Corporation Indianapolis 6, Indiana Attention: J. D. Dunlop II	1
Aracon Laboratories Virginia Road Concord, Massachusetts Attention: S. Ruby	1
Argonne National Laboratory 9700 South Cass Avenue Argonne, Illinois Attention: Aaron J. Ulrich	1

Illinois Institute of Technology
Research Institute
10 West 35th Street
Chicago 16, Illinois
Attention: D. W. Levinson 1

Atomics International
P. O. Box 309
Canoga Park, California
Attention: Robert C. Allen 1
Charles K. Smith 1

The Babcock & Wilcox Company
1201 Kemper Street
Lynchburg, Virginia
Attention: Russell M. Ball 1

Battelle Memorial Institute
505 King Avenue
Columbus 1, Ohio
Attention: David Dingee 1
Don Keller 1

The Bendix Corporation
Research Laboratories Division
Northwestern Highway
Detroit 35, Michigan
Attention: W. M. Spurgeon 1

Bureau of Ships
Department of the Navy
Washington 25, D. C.
Attention: B. B. Rosenbaum 1
John Huth 1

Consolidated Controls Corporation
Bethel, Connecticut
Attention: David Mends 1

Mr. John McNeil
Market Development Manager
Research Division
Allis-Chalmers Manufacturing Company
Post Office Box 512
Milwaukee, Wisconsin 1

Douglas Aircraft Company
Missile & Space Engineering
Nuclear Research (AZ-260)
3000 Ocean Park
Santa Monica, California
Attention: A. Del Grosso 1

Electro-Optical Systems, Incorporated
300 North Halstead Avenue
Pasadena, California
Attention: A. Jensen 1

Ford Instrument Company
32-36 47th Avenue
Long Island City, New York
Attention: A. Medica

General Atomic
P. O. Box 608
San Diego 12, California
Attention: R. W. Pidd 1
L. Yang 1
A. Weinberg 1

General Electric Company
Missile & Space Vehicle Department
3198 Chestnut Street
Philadelphia 4, Pennsylvania
Attention: Library 1

General Electric Company
Knolls Atomic Power Laboratory
Schenectady, New York
Attention: R. Ehrlich 1

General Electric Company
Power Tube Division
One River Road
Schenectady 5, New York
Attention: D. L. Schaefer 1

General Electric Company
Nuclear Materials & Propulsion Operation
P. O. Box 15132
Cincinnati 15, Ohio
Attention: J. A. McGurty 1

General Electric Company
Research Laboratory
Schenectady, New York
Attention: Volney C. Wilson 1
John Houston 1

General Electric Company
Special Purpose Nuclear System Operations
Vallecitos Atomic Laboratory
P. O. Box 846
Pleasanton, California
Attention: E. Blue 1
B. Voorhees 1

General Motors Corporation
Research Laboratories
Warren, Michigan
Attention: F. E. Jamerson 1

Hughes Research Laboratories
3011 Malibu Canyon Road
Malibu, California
Attention: R. C. Knechtli 1

Institute for Defense Analyses
400 Army-Navy Drive
Arlington, Virginia 22202
Attention: R. C. Hamilton 1

Jet Propulsion Laboratory
California Institute of Technology
4800 Oak Grove Drive
Pasadena, California
Attention: Peter Rouklove 1
Library 1

Los Alamos Scientific Laboratory
P. O. Box 1663
Los Alamos, New Mexico
Attention: G. M. Grover 1
Walter Reichelt 1

Marquardt Corporation
Astro Division
16555 Saticoy Street
Van Nuys, California
Attention: A. N. Thomas 1

Martin - Nuclear
Division of Martin-Marietta Corporation
P. O. Box 5042
Middle River 3, Maryland
Attention: J. Levedahl 1

Massachusetts Institute of Technology
Cambridge, Massachusetts
Attention: Robert E. Stickney 1
Elias P. Gyftopolous 1

National Aeronautics & Space Administration
Manned Spacecraft Center
Houston, Texas
Attention: J. D. Murrell 1

National Aeronautics & Space Administration
600 Independence Avenue, N. W.
Washington 25, D. C.
Attention: Fred Schulman 1
James J. Lynch 1
H. Harrison 1
Arvin Smith 1

National Aeronautics & Space Administration
Lewis Research Center
21000 Brookpark Road
Cleveland, Ohio 44135
Attention: Roland Breitwieser (C&EC) 1
Robert Migra (NRD) 1
Bernard Lubarsky (SPSD) 1
James J. Ward (SPSD) 1
Herman Schwartz (SPSD) 1
C. Walker (SPSPS) 1
R. Mather (SPSD) 1
H. E. Nastelin (SPSD) 3
John J. Weber (TUO) 1

National Aeronautics & Space Administration
Marshall Space Flight Center
Huntsville, Alabama
Attention: Library 1

National Aeronautics & Space Administration Scientific & Technical Information Facility P. O. Box 5700 Bethesda 14, Maryland Attention: NASA Representative	2 Copies & 1 Reproduction
National Aeronautics & Space Administration Goddard Space Flight Center Greenbelt, Maryland Attention: Joseph Epstein	1
National Bureau of Standards Washington, D. C. Attention: Library	1
Oak Ridge National Laboratory Oak Ridge, Tennessee Attention: Library	1
Office of Naval Research Power Branch Department of the Navy Washington 25, D. C. Attention: Cdr. J. J. Connelly, Jr.	1
Power Information Center University of Pennsylvania Moore School Building 200 South 33rd Street Philadelphia 4, Pennsylvania	1
Pratt & Whitney Aircraft Corporation East Hartford 8, Connecticut Attention: William Lueckel	1
Franz Harter	1
Radio Corporation of America Electron Tube Division Lancaster, Pennsylvania Attention: Fred Block	1
Radio Corporation of America David Sarnoff Research Center Princeton, New Jersey Attention: Karl G. Hernqvist	1
Paul Rappaport	1

The Rand Corporation
1700 Main Street
Santa Monica, California
Attention: Librarian 1

Republic Aviation Corporation
Farmingdale, Long Island, New York
Attention: Alfred Schock 1

Space Technology Laboratories
Los Angeles 45, California
Attention: Kenneth K. Tang 1

Texas Instruments, Incorporated
P. O. Box 5474
Dallas, Texas
Attention: R. A. Chapman 1

Thermo Electron Engineering Corporation
85 First Avenue
Waltham 54, Massachusetts
Attention: George Hatsopoulos 1
S. Kitrilakis 1

Thompson Ramo Wooldridge, Incorporated
7209 Platt Avenue
Cleveland, Ohio
Attention: W. J. Leovic 1

United Nuclear Corporation
Five New Street
White Plains, New York
Attention: Al Strasser 1

U. S. Army Signal R & D Laboratory
Fort Monmouth, New Jersey
Attention: Emil Kittil 1

U. S. Atomic Energy Commission
Division of Reactor Development
Washington 25, D. C.
Attention: Direct Conversion Branch 1

U. S. Atomic Energy Commission
Technical Reports Library
Washington 25, D. C.
Attention: J. M. O'Leary 3

U. S. Atomic Energy Commission Department of Technical Information Extension P. O. Box 62 Oak Ridge, Tennessee	3
U. S. Atomic Energy Commission San Francisco Operations Office 2111 Bancroft Way Berkeley 4, California Attention: Reactor Division	1
U. S. Naval Research Laboratory Washington 25, D. C. Attention: George Haas	1
Library	1
Defense Research Corporation P. O. Box 3587 Santa Barbara, California Attention: Harold W. Lewis	1
Westinghouse Electric Corporation Research Laboratories Pittsburgh, Pennsylvania Attention: R. J. Zollweg	1
The Boeing Company Seattle, Washington Attention: Howard L. Steele	1
Varian Associates 611 Hansen Way Palo Alto, California Attention: Ira Weissman	1